Design and characterization of xylitol based hydrogel systems

A THESIS PRESENTED BY

P. MADHAV VINODH

TO

SREE CHITRA TIRUNAL INSTITUTE FOR MEDICAL
SCIENCES AND TECHNOLOGY
THIRUVANANTHAPURAM
INDIA

IN PARTIAL FULFILMENT OF THE REQUIREMENTS
FOR THE AWARD OF
MASTERS IN PHILOSOPHY

2014

DECLARATION

I, P. Madhav Vinodh, hereby certify that I had personally carried out the work depicted in the thesis entitled, ***"Design and characterization of xylitol based injectable hydrogel system",*** except where due acknowledgment has been made in the text. No part of the thesis has been submitted for the award of any other degree or diploma prior to this date.

Thiruvananthapuram
7-07-2014

P.Madhav Vinodh
Reg No: M.Phil/2013/03
Roll No: 6531

SREE CHITRA TIRUNAL INSTITUTE FOR MEDICAL SCIENCES & TECHNOLOGY, TRIVANDRUM

Thiruvananthapuram – 695011, INDIA
(An Institute of National Importance under Govt. of India)
Phone-(91)0471-2520248 Fax-(91)0471-2341814
Email: jayabalan@sctimst.ac.in Web site – www.sctimst.ac.in

CERTIFICATE

This is to certify that Mr. P.Madhav Vinodh, in the Polymer Division of this institute has fulfilled the requirements prescribed for the M.Phil degree of the Sree Chitra Tirunal Institute for Medical Sciences and Technology, Thiruvananthapuram. The thesis entitled, ***"Design and characterization of xylitol based injectable hydrogel systems"*** was carried out under my direct supervision. No part of the thesis was submitted for the award of any degree or diploma prior to this date.

Thiruvananthapuram
23-06-2014

Dr. M Jayabalan PhD, DSc, FABMS
(Research Supervisor)

Scientist G & Head
Polymer Division
BMT wing, SCTIMST,
Thiruvananthapuram

The thesis entitled

"Design and Characterization of Xylitol based hydrogel systems".

Submitted by

P. Madhav Vinodh

for the degree of

Masters in Philosophy

SREE CHITRA TIRUNAL INSTITUTE
FOR MEDICAL SCIENCES AND TECHNOLOGY,
THIRUVANANTHAPURAM - 695011

is evaluated and approved by

…….	……..
Dr. M Jayabalan. PhD. DSc. Scientist-In-Charge, Polymer Division (Research Supervisor)	Examiner

ACKNOWLEDGEMENT

I express my deep sense of gratitude and respect to Dr.Jayabalan, Scientist-G & Head, Polymer Science Division for guiding me and extending the opportunity to do research and encouraging me in all grounds by showering his fatherly suggestion time to time.

My heartfelt gratitude to Dr. Shivaram Selvam, INSPIRE Faculty for monitoring my work.

My sincere thanks to Dr. Sunita Prem Victor, Chitra high value fellow, Polymer divion, for her valuabe suggestion and guidance.

I thank Prof. Tushar Jana, School of chemistry, University of Hyderabad, for extending his NMR facility to carry out NMR analysis on samples.

I thank Mr.Willipaul, Scientific Officer, FADDS, BMT Wing for extending the lab facilities to carryout viscometry and spectrophotometric analysis and Fluorescent microscopy studies

I thank my lab mates Mr. Finosh(Ph.D student), Mr. Vineeth(Ph.D student), Ms. Remya(Ph.D student) for their constant support and encouragement.

Heartfelt thanks to all my friends and well wishers who supported me all through the year: Anand&Aravind, kamaruddin, Elsa; Rohan Thakur, Almas Kiran Shamim; Dr. Shammi, Merlin, Neeraj, Soumya, Madhura, Anil, Venkatesh, and my seniors.

Last but not least I thank all the faculty members, Technical staff, Admin. Staff and the entire chitra family for all the learning, fun and joy.

Madhav…

Contents

1. INTRODUCTION

1.1 Hydrogels

Hydrogels are 3-dimensional water swollen matrices formed by the network of hydrophilic polymer chains that are cross-linked either physically or covalently and can be cast into any size and shape (Hoffman *et al*., 2001; Gulrez *et al*., 2003; Saha 2011; Annabi *et al*., 2014; Pal *et al*., 2009; Seliktar 2012). While porosity, swelling, mechanical and surface characteristics of hydrogels are predominantly tunable and scalable making them apt candidates for tissue engineering applications, the biocompatible and biodegradable nature qualifies them to be widely applicable in the biomedical research and patient care (Nguyen *et al.*, 2010; Rodrigues *et al.*, 2012; Yu *et al.*, 2008; Patenaude *et al.*, 2014). Some of the early innovations like soft contact lenses made form PHEMA and fibrin glue as surgical adhesive aide turned out as highly successful products in biomedical industry (Saha, 2011). The wound care applications of hydrogels are well known and are today available under various brand names as commercial products in the form of gels or gauze impregnated. Hydrogels of polyurethane, poly(vinyl pyrrolidone), xanthan, hyaluronan etc are available under various brand names which were clinically successful (Gulrez *et al*., 2003).

1.2. Classification of hydrogels

The broad range of hydrogels can be classified based on various criteria. Primarily, basing on gelation or crosslinking, hydrogels are classified into physical and covalent gels. Based on polymeric composition they can be either natural, synthetic or both (biosynthetic) (Hoffman *et al*., 2001; Gulrez *et al*., 2003; Seliktar 2012). Mechanisms of physical crosslinking are hydrogen bond formation, electrostatic interactions or hydrophobic interactions which hold individual polymers to form network. As all of these interactions are either pH, or temeperature sensitive, the polymeric networks can be easily disrupted by changing the physical conditions like ionic strength or stress (Hoffman *et al*., 2001). Hence they are also called as “reversible” gels with stimuli responsive characteristics. Unlike physical, hydrogels follow covalent crosslinking mechanism to form polymer networks. The chemical gelation occurs majorly via chemical crosslinking of polymers. Table 1 details the classification of hydrogels with examples.

Synthetic polymer based hydrogels has also been for a variety of tissue engineering applications due to their versatility in controlling physical and biochemical properties, stiffness, water content and cell adhesion. They are easy to cast and handle and are cost-effective compared to the natural polymers. However, their biocompatibility and possible inflammatory reactions are challenging issues. Poly(ethylene glycol) (PEG), a water-soluble polymer synthesized by the ring-opening polymerization of ethylene oxide, is biocompatible and has been approved by the FDA. PEG is widely used as scaffold for various tissue engineering applications due to its anti-fouling

properties and low risk of inflammation. The conjugation of cell adhesive peptides or proteins and incorporating growth factors can be employed to increase the cell adhesion on these PEG based hydrogels (Li *et al*., 2011).

Synthetic polyesters have better response for tissue engineering applications due to their controlled degradation and sustenance of mechanical properties (Wang et al., 2010). But the use of these biodegradable polyesters in soft tissue engineering is limited due to elastic deformation, acidic degradation products, absence of cell recognition signals and so on (Serrano *et al*., 2010). For example synthetic unsaturated polyester, poly(propylene fumarate) (PPF) gained importance due to its mechanical stability and bioresorption profile. In the biological environment, PPF undergo enzymatic degradation to form the TCA cycle intermediate, fumaric acid, which can enter TCA cycle. The other degradation product, 1,2-propanediol is commonly used as a diluent in pharmaceutical products. PPF-based biodegradable composites and hydrogels were investigated for orthopedic and tissue engineering applications (Jayabalan *et al*., 2009). Sebacic acid, the C10 dicarboxylic acid, is a natural metabolite formed by β-oxidation of long chain carboxylic acids and ω-oxidation of medium and short chain fatty acids. Since sebacic acid undergo cellular metabolism to form the TCA intermediate succinate, its use in cardiac tissue engineering hydrogels offers a safer application (Sailakshmi *et al.*, 2013). Mannitol is the sugar alcohol formed from the hexose sugar mannose and is commonly used as food ingredients (Mäkinen and Hämäläinen, 1985). Mannitol can enter glycolytic pathway by the formation mannose by mannitol dehydrogenase enzyme, which can then

form either glucose or fructose. Fumaric acid, the TCA intermediate, based polyesters were already proven to be biocompatible and non-toxic for tissue engineering applications (Jayabalan *et al*., 2000).

Table 1: Classification of hydrogels

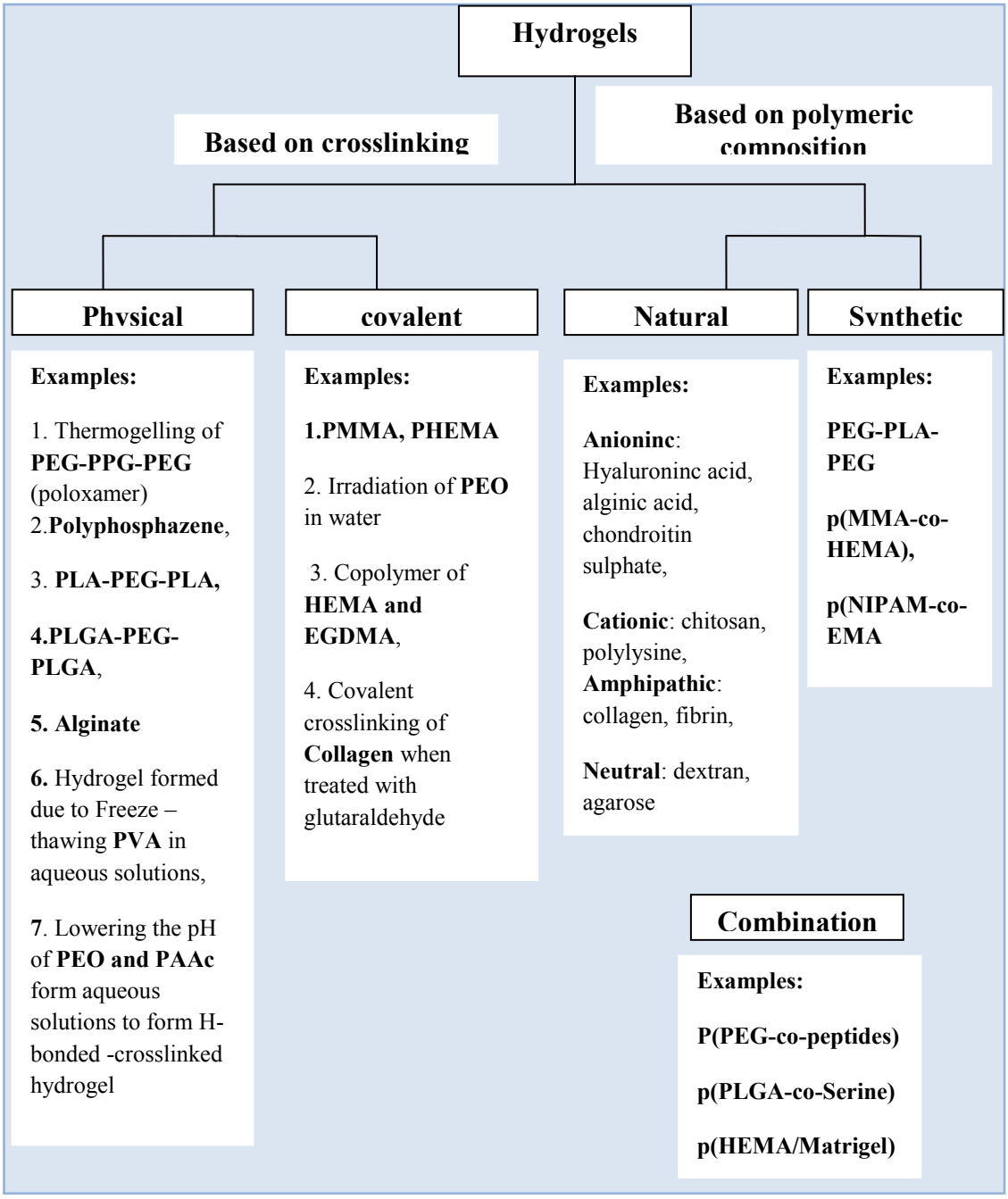

Gelation kinetics and temperature greatly influences various properties of gels like crosslinking density, equilibrium swelling and mechanical strength (Hoffman *et al*., 2001; Gulrez *et al*., 2003).

1.3. General characteristics of hydrogels

1.3.1. Water holding capacity

Water holding capacity of hydrogels is a unique character that contributes to the “swelling” property. Water molecules in hydrogel can be present three forms as “primary bound water” which interact with hydrophilic groups, “secondary bound water” that interacts with hydrophobic groups, and free water that fills the spaces between the networks. Swelling characteristics imparts free diffusion of cargo and gases to the encapsulated cells (Hoffman *et al*., 2001; Gulrez *et al*., 2003).

1.3.2. Mechanical strength

Mechanical strength is mainly governed by gelation kinetics and crosslinking density (Pal *et al*., 2009). One of the major objectives of hydrogel designs is to match the mechanical properties of the native tissue which will integrate with tissue and promotes cell differentiation and proliferation and tissue infiltration. For example just varying the stiffness of polyacryamide gels, they can be fabricated into matrices that are are lineage specific: neurogenic(1-2Kpa), or myogenic(8-17Kpa), or osteogenic (24-40Kpa) gels (Seliktar 2012). Fibroblasts and endothelial cells adhere to a stiff surface (>

2−3 kPa) show significant spreading and form more actin stress fibers than on a softer surface (< 2−3 kPa). Migration is affected by stiffness due to anisotropic rigidity which can induce directional epithelial growth and guide cell migration along the direction of strongest rigidity. Hydrogel stiffness is described by its elastic modulus, which is a measure of the strain when stress is applied to a material and can be measured via rheology measurements or indentation experiments. In rheology, a controlled stress is applied to the sample of interest and the corresponding strain is measured, or a controlled strain is induc ed and the applied stress is measured. Since the force is applied to the entire sample, the resulting stiffness is an average value of the bulk stiffness. In contrast, indentation studies on hydrogels measure elasticity at the mm to μ m scale. Samples are indented by small probes and the correlation between the applied force and resulting indentation is measured.

Despite the ability to probe hydrogel elasticity with high resolution, for example by using an atomic force microscope with a colloidal probe, in homogeneities in the polymer network on the length-scale of the probe can result in significant deviations of elasticity data from those obtained by rheology. Moreover, hydrogel samples can adhere to the probe during retraction, affecting the outcome of the measurement if this is not corrected for in the chosen model. The relationship between stress and strain in a hydrogel material can be described by the rubber elasticity model. Both natural and synthetic hydrogels show a non-linear stress-strain relation, but many natural materials, including fibrin, collagen and actin present a unique viscoelastic property, where the elastic modulus strongly increases the more

the material is deformed. This so-called strain-stiffening phenomenon could be an important factor in studying cell-matrix interactions as the cells can locally and globally stiffen the gel. Synthetic hydrogel of poly(isocyanopeptides) has been developed that possesses this fascinating physical property. Fully swollen synthetic hydrogels usually consist of hydrophilic polymer chains that are fully extended in the aqueous media (*Julian Thiele & Yujie Ma, 2014).*

1.3.3. Porosity:

The porosity of the material is an important environmental factor for cells and their viability, as large pores facilitate the efficient transport of nutrients, carbon dioxide and oxygen. In 3D, cell migration is fastest at pore diameters that match, or are slightly below, the diameter of polarized cells; migration speeds decrease in large pore size matrices due to the loss of cell-matrix interactions; but pore sizes much smaller than cell sizes trap cells in a physical ‘cage’ and reduce cell migration.

Porosity refers to the maximum size of solutes that can diffuse in a hydrogel, which can be described by the mesh size that quantifies the average linear distance between crosslinks and provides a measure of the space available between the macromolecular chains. The mesh size is an estimation of the average pore size assuming ideal crosslinking of the hydrogel molecules. However, a real hydrogel matrix usually contains larger and smaller pores due to non-crosslinked polymer chains contributing to an

increase in effective pore size, while polymer chain entanglements decrease the pore size (*Julian Thiele & Yujie Ma, 2014)*. The mesh size of hydrogels can be estimated by a number of experimental techniques, like mercury intrusion porosimetry(MIP), fluorescence microscopy using dextran probes and scanning electron microscopy (SEM), While MIP is a rather standard method for porosity characterization, the hydrogel sample is kept under vacuum and thus the polymer chains are fully collapsed. Hydrogels samples for cryo-SEM measurements are also subjected to vacuum and are thus also at least partially collapsed. Diffusion of fluorescent probes of precise molecular weight can be influenced by their interactions with the polymer host.

To obtain the pore size of a hydrogel in a theoretical way, one has to know the swollen polymer volume fraction. This parameter is derived from the swelling ratio of a hydrogel from the dried to solvated state. The porosity of a hydrogel can then be predicted by the Flory-Rehner theory, which describes the thermodynamics of the equilibrium swelling of a crosslinked polymer network in a fluidic environment. The theory describes the entropy of mixing of a solvent and a polymer network such as a hydrogel. The Flory-Rehner equation takes into account the average molecular weight between the crosslinks, which is closely related to the polymer volume fraction in the swollen state as well as the solvent-polymer interaction parameter (Hoffman *et al*., 2001; Gulrez *et al*., 2003; Seliktar 2012) In complex situations when ionic interactions also play a role,a more sophisticated version of this equation can be used. However, as the crosslinking of a polymer network is a random process, the polymer chain assembly inside the network is not uniform. By

treating the polymer chains as Gaussian chains, their assembly can described by a Gaussian distribution function with sufficient accuracy.

On the micro scale, porosity of a hydrogel can be controlled using solvent phase inversion whereas on the macro scale pore size can be varied by encapsulating inorganic particles that can be selectively dissolved after crosslinking the hydrogel matrix. Other methods include stratifying hydrogel samples onto surfaces with controlled porosity as well as by growing salt crystals inside a hydrogel solution upon crosslinking. (*Julian Thiele & Yujie Ma, 2014)*

1.3.4. Biocompatibility & Biodegradability

Biocompatibility is the third most important characteristic property of hydrogel. Hydrogels are biocompatible when they are non-toxic and donot elicit immune reaction, they degrade in the host system and degradation products must be harmless and should be bio-resorbable. In general, hydrophilic surface of hydrogel has alow interfacial free energy when in contact with body fluids, which results in a low tendency for proteins and cells to adhere to these surfaces. Moreover, the soft and rubbery nature of hydrogels minimizes irritation to surrounding tissue (Hoffman *et al*., 2001; Gulrez *et al*., 2003).

Many natural matrices such as collagen or fibrin hydrogels are enzymatically degradable, enabling cells to degrade and remodel their

surrounding environment. As the pore size of many hydrogels based on natural materials is usually only slightly smaller than the size of a typical mammalian cell. The cells can spread, grow and migrate by remodeling the polymer matrix without degrading the material. For hydrogels based on synthetic materials, which usually have pore sizes much smaller than the typical size of mammalian cells, degradability is crucial since the cells require space to spread, grow and proliferate. The importance of matrix degradability has been highlighted in studies of cellular invasion of artificial matrices. It was found that fibroblasts could invade adhesive and degradable synthetic hydrogel and that invasion distances increased approximately linearly with culture time. Similarly, poly(ethylene glycol) hydrogels were described, either containing adhesion sites or protease sensitive crosslinkers, or both. Cell elongation was observed only in networks that contained both active adhesion ligands and degradable substrates. Digital time-lapse microscopy was used to quantify 3D cell migration. Within hydrogels that were functionalized with proteins for adhesion, cells extensively migrated, proliferated and formed interconnected cellular networks only when the scaffold material was sensitive for degradation.

Synthetic materials are often used for migration studies as their degree of degradability can be controlled and degradable materials can easily be compared to non-degradable materials. Alternatively, the degradability of hydrogels based on pure natural polymers can be restricted synthetically. Increasing density of non-degradable crosslinks limits cell spreading in hydrogels that were patterned using sequential crosslinking. A primary

crosslinking reaction formed by hyaluronic acid hydrogel with degradable peptide crosslinks; subsequently a UV light-induced radical reaction spatially introduced a non-degradable network. This property affected the morphology and eventually the fate of human MSCs cultured within these hydrogels. (*Julian Thiele & Yujie Ma, 2014).*

1.4. Injectable Hydrogels (IH)

In the case of tissue or organ damage, the surgical intervention with the use of hydrogel based tissue fillers and adhesives for regenerative therapy and drug carriers for sustained drug release is increasingly growing (Annabi *et al*., 2014). Mostly such hydrogels are aqueous solutions that are either cell encapsulated or drug loaded and intended for body administration via non-surgical procedures, by simple syringe delivery mode. Once injected at the site of organ or tissue defect, the hydrogel (i.e.) in sol state fills the geometry of the defect and crosslink to provide 3D microenvironment that holds and allows the flow of cargo or aids in cell delivery across the defect, thus serving in its repair meachanism (Nguyen *et al*., 2007; Li *et al*., 2012; Yu and Ding, 2008).

Some of the successful injectable hydrogel products to date are based on naturally available hyaluronic acid, alginate, gelatin, fibrin or synthetic polymers, such as polyvinyl alcohol, polyethylene glycol (PEG), polypropylene fumarate, and polylactones. Injectable hydrogel products like Hylaform gel (HA based) for deep skin defects and facial wrinkles, Sculptra(poly-(l-Lactic acid based) gel and Bio-Alcamid(poly-alkyl-imide based) for deep tissue

defects, Aquamid (Polyacrylamide based) and Reviderma(dextran beads in hylan gel) for lip augumentation etc are commercially available (Nguyen *et al*., 2007; Li *et al*., 2012; Yu and Ding, 2008).

Based on major criteria for creating 3D microenvironment and syringebility, certain design principles were laid down by Helena *et al.,* 2012 and Ding *et al.,* 2008. According to them, injectable hydrogels must be:

(i) Made up of biocompatible and biodegradable materials that degrade to products that are biocompatible. The degradation should provide space for tissue infiltration.

(ii) The polymer mixture or gel precursors must be water soluble and of sufficiently low viscosity so as to ensure homogeneous dispersion of drugs/cells and should pass through the fine needle of syringe of size at least 25G.

(iii) Gelation must be mild and shouldn't be toxic or overheating. It should begin only after complete injection to the target site and can occur via physical or chemical cross-linking mechanism.

(iv) Should match the specific properties of target tissue like mechanical strength, electrical conductivity.

(v) Should possess good porosity and pore interconnectivity to allow cell activity and diffusion of oxygen and nutrients.

1.5. Covalently crosslinked injectable hydrogels

Injectable hydrogels based on type of in-situ gelation they can be physical or covalent hydrogels. In turn polymer constituents of injectable systems can be either natural or synthetic. Physical hydrogels are mainly physiological responsive, and gel under such conditions. As discussed earlier, the changes in pH, ionic strength, electric field can also trigger the gelation. For e.g Hyaluronic acid, functionalized with amines, can crosslink in water, mainly due to hydrophobic interactions (Annabi *et al*., 2014; Yu and Ding, 2008) and is available as commercial product under various brand names. Sodium alginates upon slow addition of calcium sulphate will eventually crosslink at the site of injection due to columbic interactions (Annabi *et al.*, 2014). Similarly, Physical hydrogels belonging to the class of thermogelling polymers like PEG-PLGA-PEG co-polymers, cellulose derivatives, chitosan, PEG-PPG are widely investigated for biocompatibility.

Physical cross-linking gels are readily acceptable by any tissue, enhancing the chances of wide applicability and do not employ complex functional group chemistry, hence the injection mixture will be simple homogeneous mixture of gel precursors, devoid of cross-linkers and initiators (Photo: UV, Chemical: APS, TEMED) other additives which are usually toxic to cells. However, certain disadvantages like gradual dilution of polymer in-vivo due to infinitely diluting physiological environment that affects mechanical stability was observed and less control over degradation/clearance, either

leading to bioaccumulation or rapid degradation was also observed in the case of thermogelling Poloxamer which reabsorbs within hours of injection even at high concentrations. Such problems can be overcome in chemical cross-linked gels, which offer large tunable and scalable properties Patenaude *et al*., 2014).

The chemical hydrogels are formed by incorporating an additional molecule that interacts with the backbone polymers to crosslink and form gel/network of polymer. Such process is triggered by addition of initiators to the reaction mixture. Such systems offer control over large properties of hydrogels like cross linking density, swelling characteristics, compression moduli and tunable gelling kinetics that suite the application/target site characteristics compared to physical hydrogels. Moreover adjusting gelation time that can avoid gelation inside the syringe is fairly feasible using such systems. The chemical hydrogels mostly use one of the following covalent cross-linking chemistry **(Table 2).**

Recently, flexible elastomeric polymers based on polyols, which contain multiple hydroxyl (-OH) groups, have been reported for soft tissue applications (Li *et al*.,2013). These elastomers are composed of non-toxic monomers which are endogenous to the body's metabolic cycle and possess rich -OH functional groups that can be potentially utilized as sites for chemical modification or biofunctionalization (Li *et al*., 2013; Bruggeman *et al*., 2010). Examples include poly (glycerol sebacate) elastomers, which were used as scaffolds for nerve, vascular, myocardial and cartilage tissue engineering, and

xylitol-based polymers, which have been developed by langer group have received considerable interest for their excellent elastic mechanical properties and enhanced biocompatibility, both *in vitro* and *in vivo* (Bruggeman *et al*., 2008 & 2010).

Similarly biosynthetic hybrid hydrogels have emerged as promising materials for three dimensional tissue growths owing to their structural, physiochemical, mechanical and biological functionalities and their controlled degradation profile. Several combinations of biosynthetic hydrogels like glycidyl methacrylate and hyaluronic acid (Leach and Schmidt, 2005), poly(ethylene glycol)–fibrinogen conjugates (Frisman et al., 2012), poly(ethylene glycol) and heparin (Welzel et al., 2011), several combinations of poly vinyl alcohol, gluteraldehyde, chitosan and dextran, polyethylene glycol–chitosan, poly acrylic acid–alginate, chitin–PLGA, PAA–chitosan, PMAA–alginate have been reported for various biomedical applications like tissue engineering (Cascone et al., 2004), drug delivery (Gayet and Fortier, 1995), gene delivery (Loh and Li, 2007) and other biomedical applications.

Table 2: Hydrogel covalent crosslinking chemistry

Cross linking mechanism	**Example of Injectable systems**[10]
via Michael 1-4 addition	Viny-sulphones funactionalized dextran crosslinked with 1,4-dithioerythritol for bone scaffold by Peng *et al*., 2013.
via di-sulphide formation	Thiolated HA hydrogel foms due to S-S linkage (Vercruysse *et al*., 1997)
via Hydrazone formation	Hydrazone-crosslinked HA based hydrogels have shown excellent biocompatibility and gelling characteristics as demonstrated by Luo *et al*., 2010, Martinez-Sanz *et al*., 2011; Ito *et al*., 2007.
via oxime formation	Aminooxy-PEG(AO-PEG) crosslinked with gluataraldehyde
via-[2+4] Diels-Alder) Cycloaddition	cross-linking of a copolymer of *N* -isopropylacrylamide, *N,N* -dimethylacrylamide, and 2-hydroxymethacrylate functionalized with *N* -maleoyl alanine **(dieneophile)** and a copolymer of *N* -isopropylacrylamide, *N,N* -dimethylacrylamide, and furfuryl methacrylate **(diene)**
Azide-Alkyne 1,3 dipolar Huisgen Cycloaddition	Crosslinking of poly(vinyl alcohol) (PVA) modified with alkyne and azide groups, give transparent gels under Cu(I) catalyst by Ossipov *et al*., 2006.

2. OBJECTIVES OF THE STUDY

In this study, the objectives were to design a water-soluble, injectable, biodegradable xylitol-based pregel formulation that can crosslink via free radical polymerization using acrylic acid as crosslinker and form as crosslinked hydrogel. It was also our aim to synthesise the injectable pregel polymer using simple one-pot condensation reaction using non-toxic monomers, such as xylitol (X), maleic acid (M) and PEG. The monomer xylitol a polyol carbohydrate containing 5 –OH groups is biocompatible and FDA approved, as it is endogenous to the carbohydrate metabolism of the human body. These monomers are widely used as an anti-cariogenic artificial sweetener in the food industry. Maleic acid, the cis-isomer of fumaric acid that is a metabolic intermediate in Krebs cycle, has been extensively employed in biomaterial design for its crosslinkable vinyl functional groups (Tran *et al*., 2009). PEG is a hydrophilic polymer that has found broad use in various medical and pharmaceutical applications, also it is known for promoting cell adhesion (Patenaude *et al*., 2014; Tran *et al*., 2009).

The following are the detailed objectives of the present study.

i. Synthesis of poly(xylitol-co-maleate-co-PEG) prepolymer (pXMP) having different mole ratio of xylitol and maleic acid.

ii. Physiochemical characterization of prepolymers

iii. Preparation of injectable pregel formulation and hydrogels

iv. Characterization of hydrogel for swelling, crosslink density, compression property and biodegradation.

v. Evaluation of cytocompatibility of hydrogels.

vi. Carry out cell encapsulation using the polymers

3. EXPERIMENTAL

3.1. Materials

Xylitol, maleic acid, acrylic acid, and diethyl ether were purchased from Merck (India). PEG (MW: 300), ammonium persulfate (APS), and tetramethylethylenediamine (TEMED) were acquired from Sigma (Bangalore, India). High glucose Dulbecco's Modified Eagle's Medium (DMEM), fetal bovine serum (FBS) and 100X antibiotic-antimycotic solution were obtained from Invitrogen (India). MTT (3-(4,5-dimethylthiazol-2-yl)-2,5-diphenyltetrazolium bromide) assay kit procured from Invitrogen.

3.2. Synthesis of poly(xylitol-co-maleate-co-PEG) prepolymer (pXMP)

The pXMP prepolymer was synthesized using the experimental setup as shown below (Figure 1). Different prepolymers with varying molar ratios (PP1, PP2 and PP3) of xylitol to maleic acid (X/M), and PEG is shown in Table 3. The constituents were weighed in a 100 ml round bottom flask and

melted at 145 °C under a constant nitrogen atmosphere for 2 h following which high vacuum was applied for 10 min. The prepolymer was cooled down to room temperature. For purification and removal unreacted monomers, about 10 g of the resin was dissolved in 20 ml of THF and added dropwise to a beaker containing 200 ml of cold diethyl ether and stirred with a magnetic stir bar for 30 min. The ether containing unreacted monomers was then decanted carefully and the purified resin was left to dry under vacuum overnight and stored at 4 °C until further use. Typical yields of pXMP after purification were found to be around 55 - 70%.

Table 3: Formulation of pXMP prepolymers

Prepolymer [Molar Ratio(X/M)]	Xylitol (gm.wt=152.15g)		Maleic acid(gm.wt=116.072)		PEG-300(gm.wt=300)	
	Wt.	Moles	Wt.	Moles	Wt.	Moles
PP1 (1:8)	3.04	0.02	18.56	0.16	12	0.04
PP2 (1:5)	4.56	0.03	17.4	0.15	12	0.04
PP3 (1:2)	9.12	0.06	13.92	0.12	12	0.04

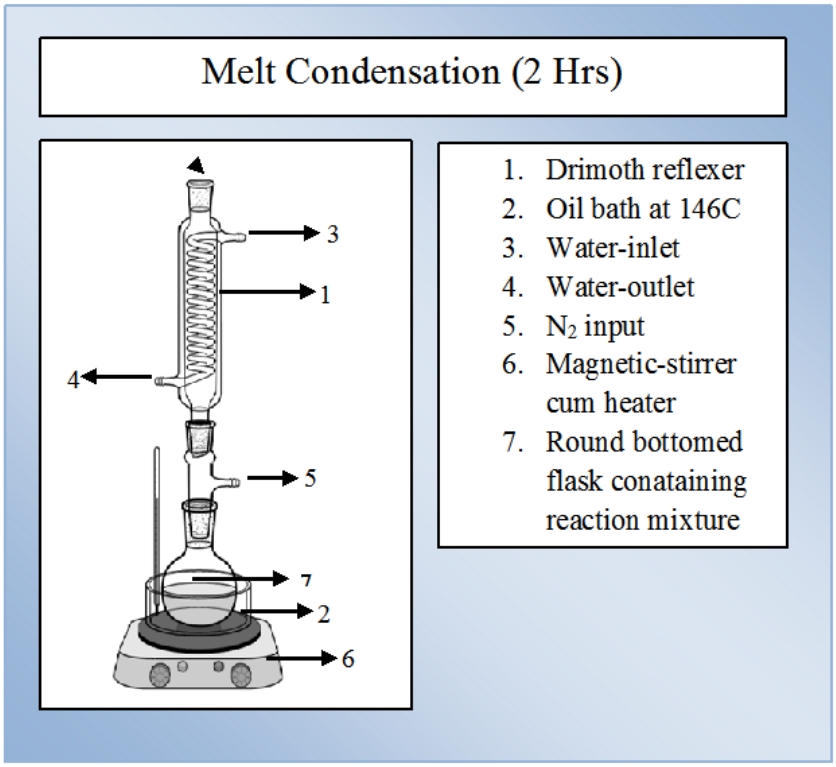

Fig. 1a. Melt condensation processes

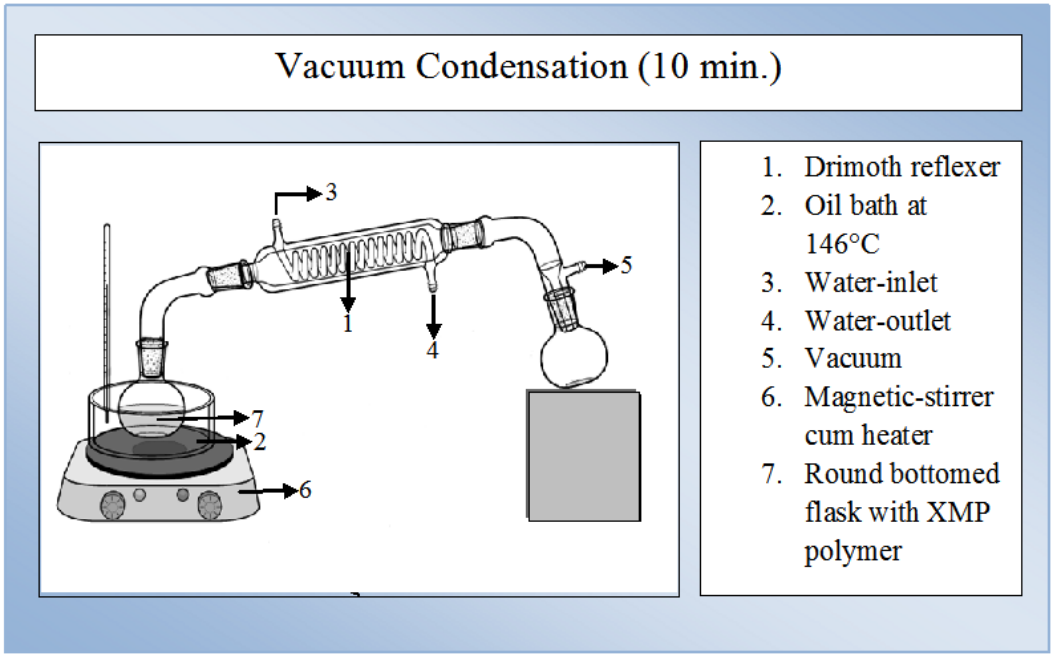

Fig. 1b. Vacuum condensation processes

3.3. Physiochemical Characterization of prepolymers

3.3.1 Determination of molecular weight

Molecular weights of the purified resin were determined using gel permeation chromatography system (Waters) using THF as the mobile phase (1 ml/min) with polystyrene beads (Mp: 100000, 9130 and 162) used as standards.

3.3.2. FTIR spectral analysis

To analyze for functional groups, samples of the synthesized polymer resins were lyophilized to remove excess water and analyzed in a Fourier transform infrared (FTIR) spectrometer (Jasco, FT/IR-4200, USA) equipped with JASCO's proprietary Spectra Manager^{TM} II crossplatform software. The viscous Freeze-dried samples were sandwiched between KBr plates and IR spectrum was recorded at room temperature. FTIR spectra were obtained in the region of 4000 - 400 cm^{-1} at a resolution of 4 cm^{-1}.

3.3.3. ^{1}H-NMR spectral analysis

For proton analysis, hydrogel samples were dissolved in dimethyl sulfoxide-d6 (DMSO-d6) and the proton nuclear magnetic resonance (^{1}H-

NMR) spectra were acquired on a Bruker AV 400 NMR spectrometer under standard quantitative conditions at ambient temperature.

3.4. Preparation of injectable pregel formulation and hydrogels

Xylitol-PEG based hydrogels were prepared using the following protocol as given in Figure 2 schematically. To 4 g of purified prepolymer, 1.05 g of acrylic acid was added and dissolved in 10 ml of distilled water. The mixture was then gently neutralized with sodium hydroxide solution (4 M) to bring pH~7.4. The pregel polymer solution was then lyophilized overnight and was dissolved again in water to a final concentration of 0.4 mg/ml.

For the preparation of hydrogel, 500µl of this pregel solution was added to a well of a 48-well tissue culture plate and polymer crosslinking was initiated by adding the redox initiators, APS (6.5 µL, 2 M) and TEMED (2 µL, 6 M) and 140µl distilled water in quick succession and mixed thoroughly. After 15 min, the disc-shaped hydrogels (12 mm diameter and 3.5 mm height) were scooped out using a clean spatula and were subsequently used for various characterization studies. The hydrogels prepared with prepolymers PP1, PP2 and PP3 are coded as R1, R2 and R3 respectively.

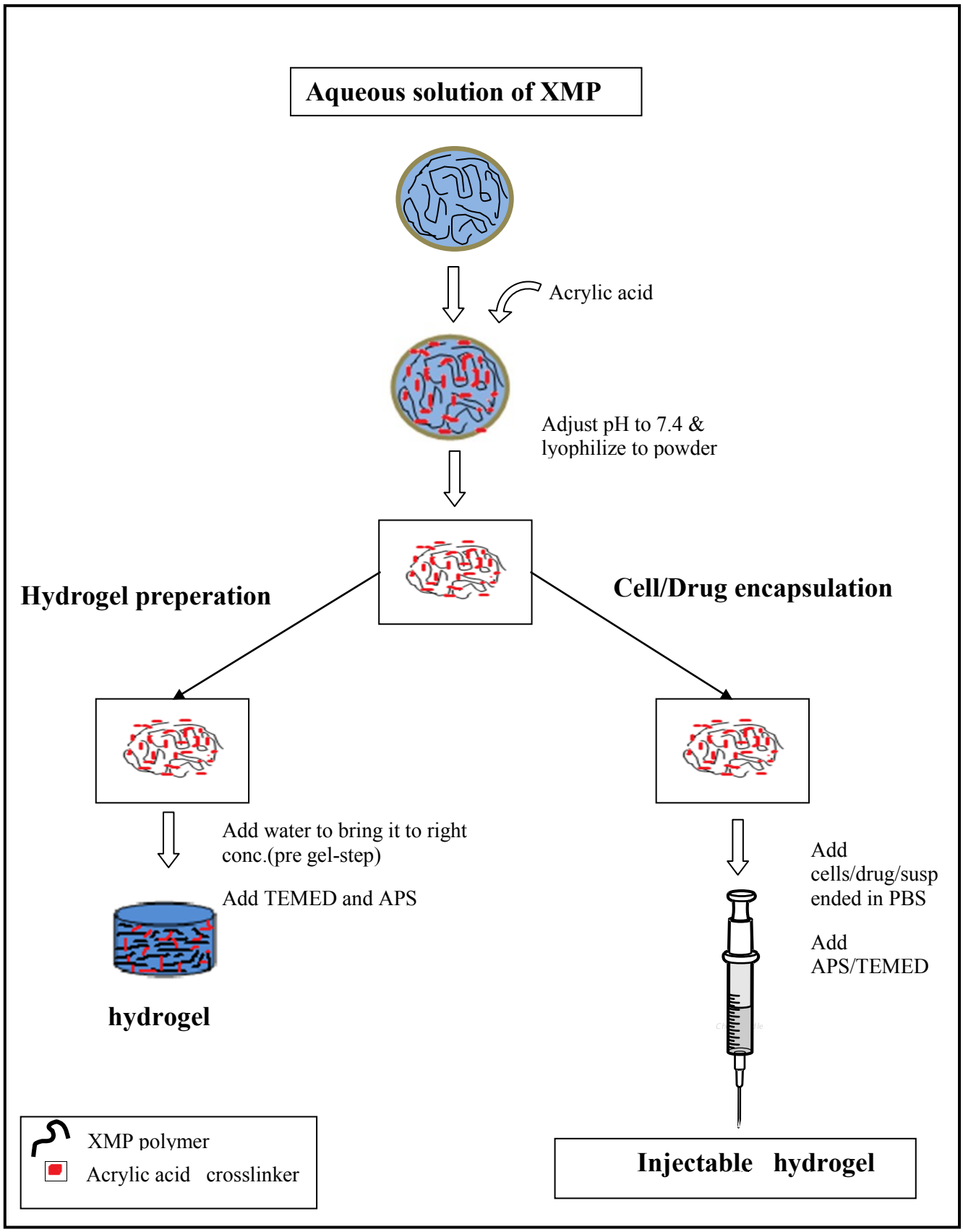

Fig. 2.Injectable Hydrogel preparation

3.5. Determination of Viscosity

Viscosity of polymer solutions in water at 37 °C was measured using a rotational viscometer (RVA-StarchMaster 2, Newport Scientific) at 200 rpm as per manufacturer's instructions.

The pregel formulation was evaluated for injectability using viscosity at measurements. 25mL of hydrogel premix was directly subjected to constant stirring at 37°C, 200rpm for 20min. using a rotational viscometer (RVA-StarchMaster 2, Newport Scientific) to measure kinematic viscocity.

3.6. Hydrogel Characterization

3.6.1. Swelling studies

Freshly synthesized hydrogels were freeze dried and incubated in PBS (pH~7.4) and SBF (pH~7.4) for 24h to calculate the percent weight swelling. Following equation was used to calculate the swelling ratio.

$$\%\text{Swelling} = \frac{W_l + W_w}{W_w} \times 100$$

where, W_L is the weight of the freeze-dried hydrogel and W_w is the weight of the swollen hydrogel incubated in phosphate buffered saline (PBS, pH~7.4) or simulated body fluid (SBF, pH~7.4).

Crosslink density and number average molecular weight between crosslinks were calculated using modified Florry-Rehner's equation (Krishna and Jayabalan, 2009).

$$\text{Crosslink density} = \frac{\left[V_r + \chi V_r^2 + \ln(1 - V_r)\right]}{dr\, V_0 \left(V_r^{1/3} - \frac{V_r}{2}\right)}$$

Molecular weight between crosslinks, $Mc = 1/\zeta$

where, χ is the Huggin's polymer-solvent interaction coefficient, assumed to be 0.34 and V is the volume fraction of the polymer in water-swollen hydrogel, which can be calculated from the swelling coefficient, ϕ using the relation,

$$V = 1/1 + \phi$$

$$\phi = W_s/W_p * D_p/D_s,$$

where, W_s is the weight of the solvent in the swollen polymer, W_p is the weight of the swollen hydrogel, D_p is the density of hydrogel and D_s is the density of water.

3.6.2. Dynamic Contact Angle Measurements (θ_w)

Thin sheets of hydrogel samples were prepared and cut into small rectangular strips (2 cm x 3 mm). The strips were incubated in clean distilled

water for 5 h to attain equilibrium swelling and dynamic contact angle measurements were then performed in water using a tensiometer (KSV Instruments Ltd., Sigma 701, Finland).

3.6.3. Compression testing

Compression testing was performed in an uniaxial compression instrument, Instron 3345 (Bioplus, India), at room temperature. Briefly, disk-shaped hydrogels (12 mm diameter and 3.5 mm height) were lyophilized and re-swelled in SBF overnight to attain equilibrium swelling. The weights and dimensions of the freeze-dried and SBF-swollen hydrogels were measured. The tests were performed using a 500 N load cell with crosshead speed of 5 mm/min^{-1}. The samples were compressed to 60% of their thickness. Compressive stress, load at break and Young's modulus were calculated using Instron's proprietary Bluehill 3 software.

3.6.4. Surface morphology

Surface morphology of the hydrogels was recorded using an environmental scanning electron microscope (ESEM). Analysis was performed on gold-coated lyophilized samples and visualized under low vacuum conditions (FEI, Quanta 200, USA).

3.6.5. Degradation

In vitro degradation of hydrogels was carried out in PBS (pH~7.4) at 37 °C for period of 7 weeks. Briefly, disk-shaped hydrogels were lyophilized, weighed, and placed in a temperature-controlled orbital shaker and constantly agitated at 100 rpm. At various time points, hydrogels were lyophilized, weighed and the mass loss was calculated using the equation below.

$$\text{Mass loss (\%)} = \frac{M_t - M_o}{M_o} \times 100$$

Where, M_o is the initial mass of the hydrogel and M_t is the mass of the hydrogel at various time points.

3.7. Biological Characterization of hydrogels

3.7.1. Protein adsorption

Protein adsorption on lyophilized hydrogel samples was evaluated using polyacrylamide gel electrophoresis (SDS-PAGE). Briefly, 10 mg of hydrogel samples were incubated in 200 µL of fresh human plasma diluted with saline (1:1). After 4 h, the tubes were centrifuged and the supernatant was carefully removed for protein analysis. Proteins in the supernatant were separated by discontinuous native-PAGE method using a previously published protocol (Laemmli, 1970). The gel was subjected to electrophoresis

(GeNei, SLM-INC-OS-250, India) at 100 V for 6h, stained in 0.5% Coomassie Brilliant Blue containing 2% v/v aqueous acetic acid solution for 30 min, and de-stained in acetic acid/methanol/water. The gel was then digitally scanned (GE Life Sciences, ImageQuant LAS 4000, India) and the densitometric values were recorded.

3.7.2. Cytotoxicity assay

Direct contact assay

Thin sheets of hydrogels were prepared on culture plate. They were swollen in PBS until equilibrium swelling. Swollen sheets were cut into small discs of 5 mm diameter. Each disc was ethanol sterilized for 24 h. The cell suspension of $5x10^6$ cells were seeded on hydrogel sheet and supplemented with DMEM medium**.** After 4 days of incubation, the cell morphology was evaluated using phase contrast microscope.

MTT assay on hydrogel extract

Lyophilized hydrogels were ethanol sterilized for 24 h and incubated in complete DMEM medium (DMEM supplemented with 10% FBS, 1X antibiotic-antimycotic solution and sodium bicarbonate) for another 24 h. The hydrogel extracts and degradation products were then diluted with DMEM into various concentrations and evaluated on L929 fibroblast cell cultures using a MTT assay kit. Briefly, 200 µL of the cell suspension containing 1 x 10^5 cells were

added to the wells of a 96-well tissue culture plate and placed in a 37 °C incubator in 5% CO_2. After attaining the desired confluency, the culture medium was removed and replaced with medium containing hydrogel extracts (200 µL). After 24 h incubation, 20 µL of stock MTT solution at 5 mg/ml concentration was added and the plate was incubated for 4 h at 37 °C. Then, 200 µL of DMSO was added to dissolve the formazan crystals and the absorbance at 570 nm was recorded using a UV/Vis microplate reader (Varian, Cary 50, USA).

3.8. Studies on cell encapsulation

The injectable pre-gel composition for cell encapsulation was made by mixing 10g of purified polymer with 2.5 mL of acrylic acid and neutralized using 4N NaOH. Then the solution was lyophilized and redissolved in 25mL of PBS. It is then filter sterilized using 0.22microns filter. 140 microL of cell suspension (about 2.5million/mL cells) was added to 500microL of the pre-gel mixture and cross-linking was initiated by adding 2microL of TEMED and 6.5microL of 2M APS. Quickly the pre-gel was pipetted to ensure mixing and 30microL was added to 1mL sterile syringe mold (tip of the syringe was break opened, and piston was positioned to an appropriate level, to act as mold and hold the hydrogel until complete setting (Khetan S AND Burdick J 2009). After 10minutes, the hydrogels were gently squeezed out and washed in PBS and trandfered to fresh 36well culture plate containing 3 ml of media.

Live dead assay was conducted after 24h of incubation using calcien and ethidium homodimer. Epifluorescence microscope (Optika SRL) with blue filter for calcien and green filter for ethidium homodimer.

3.9.Statistical analysis

All experiments were carried out with of 5 or 6 samples from each group. The values are presented as means ± standard deviations using online calculator, Statistics Calculator version-3 beta. The level of significance was set at $p < 0.05$ for all calculations.

4. RESULTS AND DISCUSSION

4.1. Synthesis of pXMP prepolymers

The prepolymer, pXMP, of three ratios PP1, PP2 and PP3 with varying feed monomer ratios as given by Table 3 were synthesized using a simple one-pot polycondensation reaction as depicted in the Figure 3. The reaction yielded a transparent to opaque viscous water-soluble polymer resin within a 2 h reaction time. The molecular weights (number average, *Mn* and weight average, *Mw*) and polydispersity index of the synthesized pXMP polymers as determined by GPC are summarized in Table 4. The analyses of molecular weights of the synthesized pXMP prepolymers confirm the oligomeric nature of the prepolymer.

Table 4: Molecular weights and polydispersity index of prepolymers

Prepolymer	M_n	M_w	*Mp*	PDI
PP1	801	1255	1315	1.57
PP2	901	1786	1305	1.98
PP3	773	1331	1066	1.72

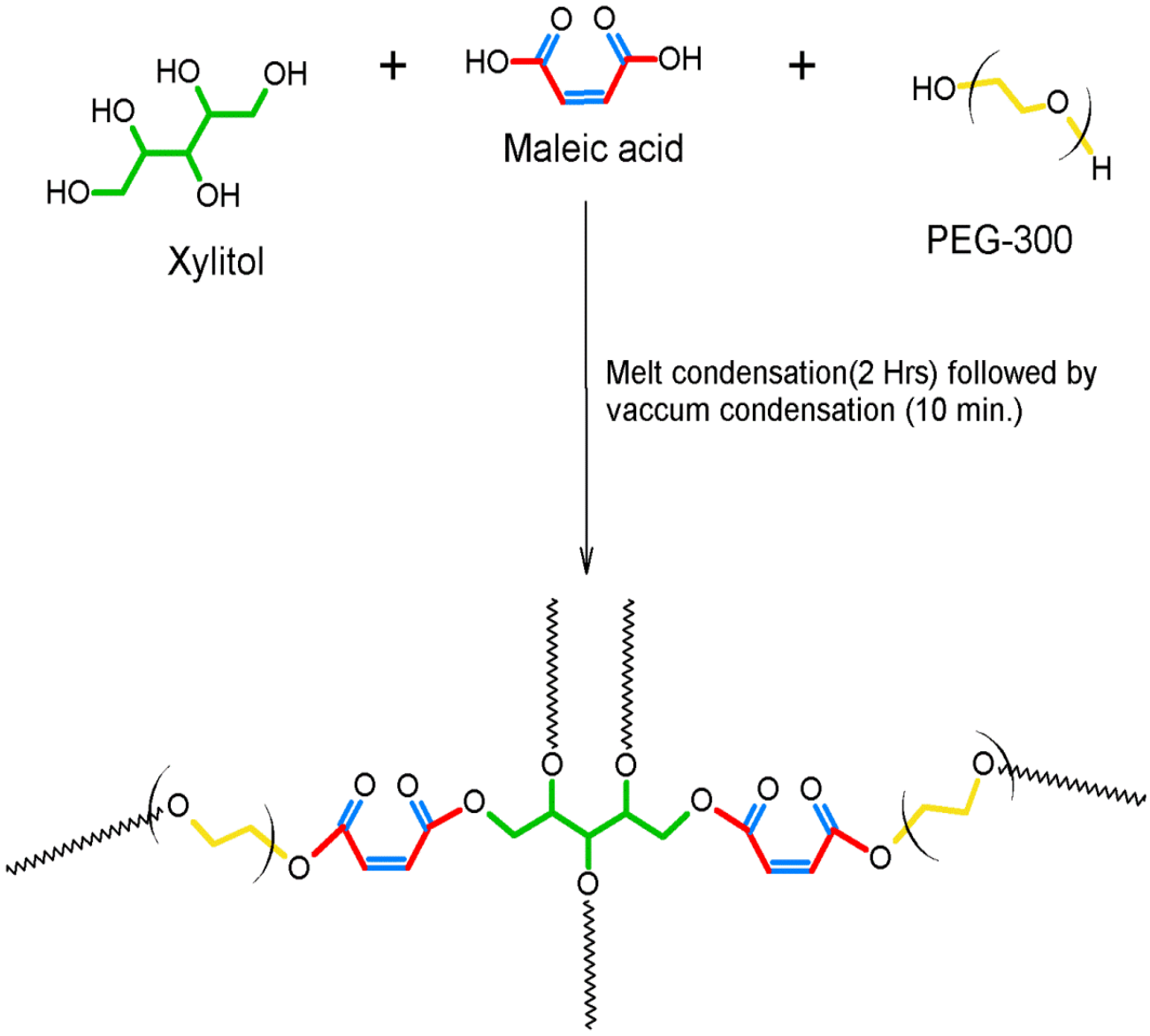

Fig. 3. Reaction Scheme of syntheses of pXMP prepolymers

4.2. Characterization of pXMP prepolymers

4.2.1. FTIR analysis

FTIR spectra confirmed the presence of degradable ester bonds, C=O at 1725 cm^{-1} and C-O at 1101 cm^{-1}, which are the characteristic stretching frequencies of carbonyl groups of ester (Figure 4).

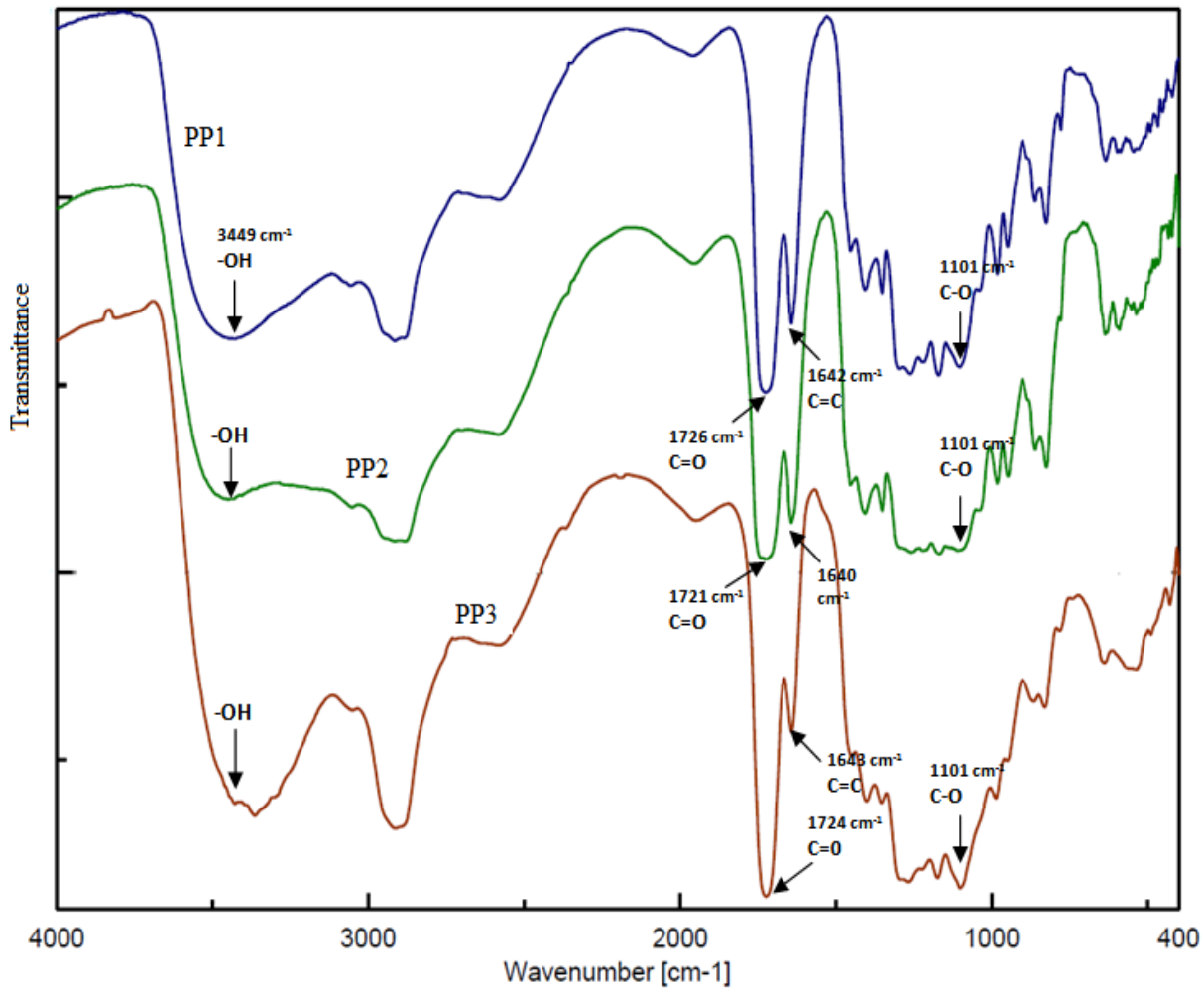

Fig. 4. FT-IR spectra of pXMP prepolymers

An intense broad band for pendant carboxylic groups at 1725 cm^{-1}, and hydroxyl group of alcohols, -OH at 3449 cm^{-1}, were also confirmed. Furthermore, the unsaturated C=C bonds in the fumarate linkage was confirmed by a strong peak at 1643 cm^{-1}.

4.2.2. ^{1}H-NMR analysis

The ^{1}H-NMR spectra displayed peaks corresponding to the -CH_2- groups in PEG (3.5 - 4.3 ppm) and the C=C maleate moieties (6.3-6.8 ppm) which is critical for crosslinking [Figures 5 (a, b, c)]. Furthermore, the -CH_2- groups in xylitol showed characteristic peaks at 6.5 ppm for all the ratios evaluated. Taken together, these results confirm the successful synthesis of pXMP with varying feed monomer compositions.

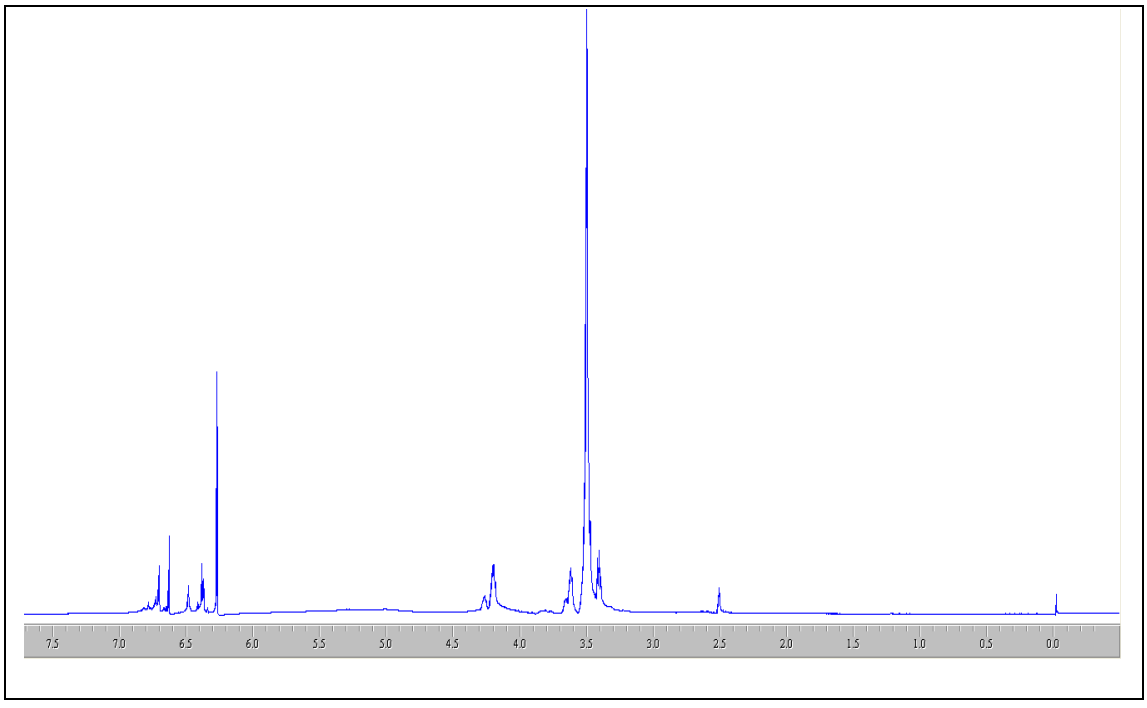

Fig. 5 (a). ^{1}H-NMR spectrum of PP1 prepolymer

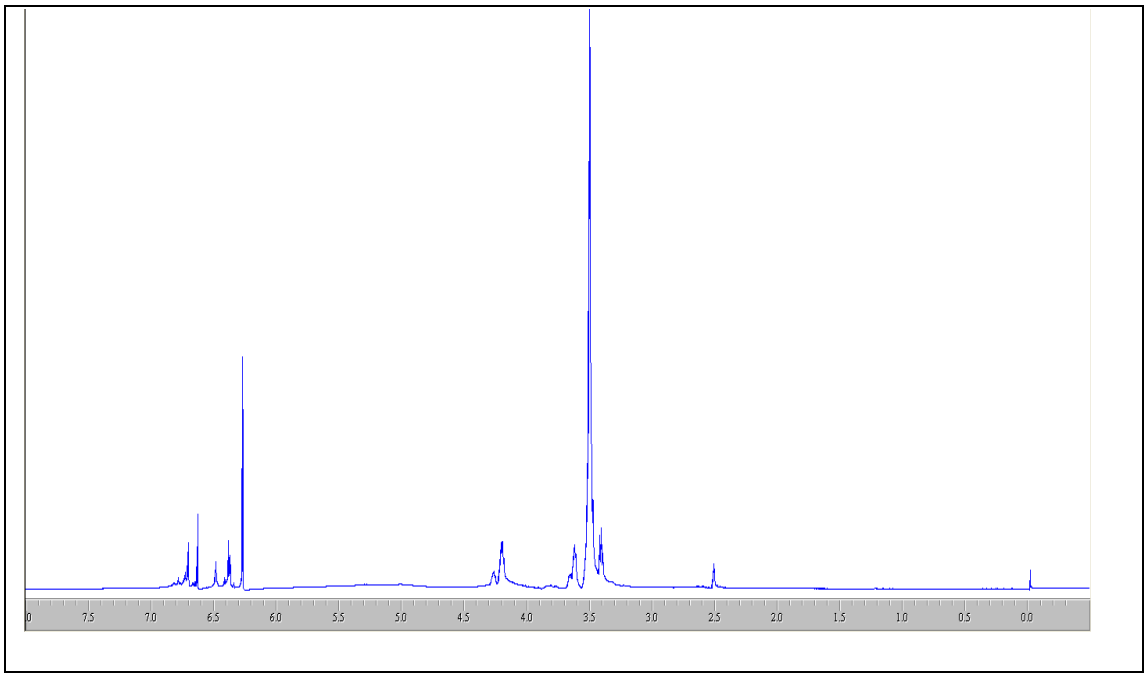

Fig. 5 (b). ^{1}H-NMR spectrum of PP2 prepolymer

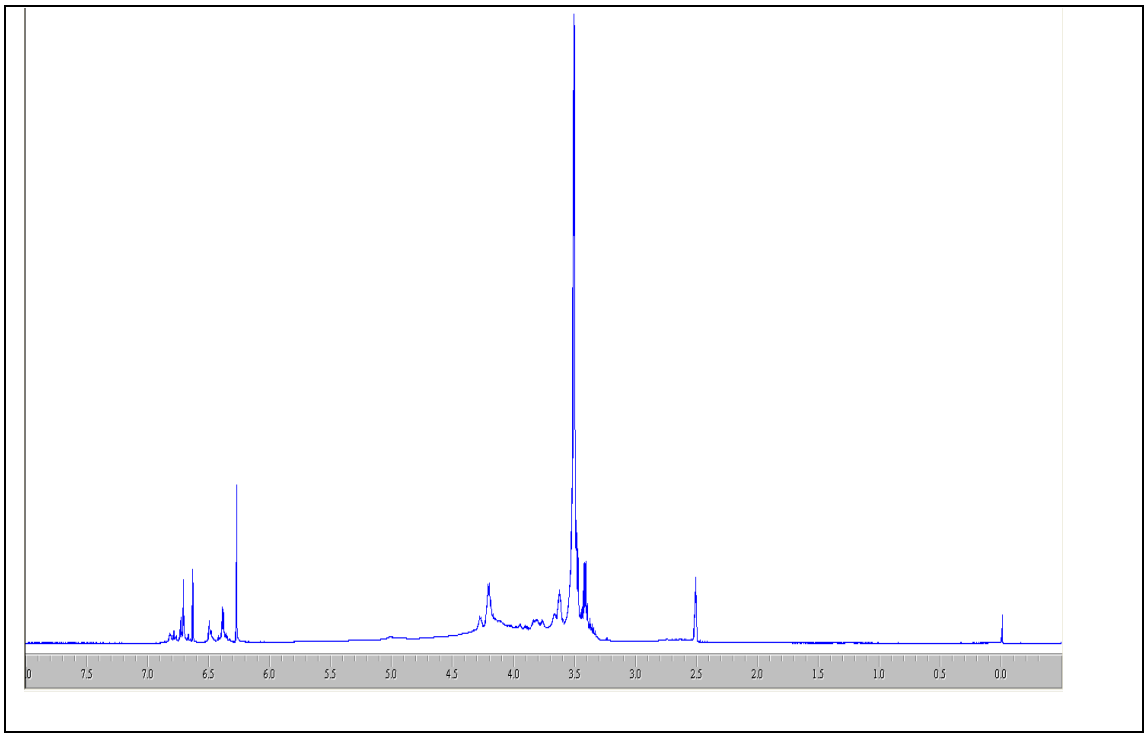

Fig. 5 (c). ^{1}H-NMR spectrum of PP3 prepolymer

4.3. Preparation of injectable pregel formulation and hydrogels

Gelation of injectable hydrogels is induced by physical interaction between polymeric chains or through chemical crosslinking via Michael addition, Schiff base, or disulphide bond formation. Compared to physical crosslinking, chemical crosslinking provides improved mechanical characteristics, tunable degradation kinetics and offers the possibility of incorporating reactive functional groups for tethering biological moieties, such as growth factors or cell-specific adhesion proteins, for guiding cell growth and tissue regeneration. To this end, bulk XMP hydrogels were prepared via free radical polymerization using the classical APS-TEMED redox initiator system. Acrylic acid, a commonly used electrophile to synthesize covalently-crosslinked hydrogels via Michael addition reaction, was used as crosslinker.

The injecatble pregel formulations of PP1, PP2 and PP3 prepolymers are coded as P-R1, P-R2 and P-R3 respectively. The pregel formulation as a free flowing liquid is shown in tissue culture tube (Figure 6a). The gel formed after crosslinking is shown in the inverted tissue culture tube (Figure 6b). The viscosity of these injectable pregel formulations are given in table 5.

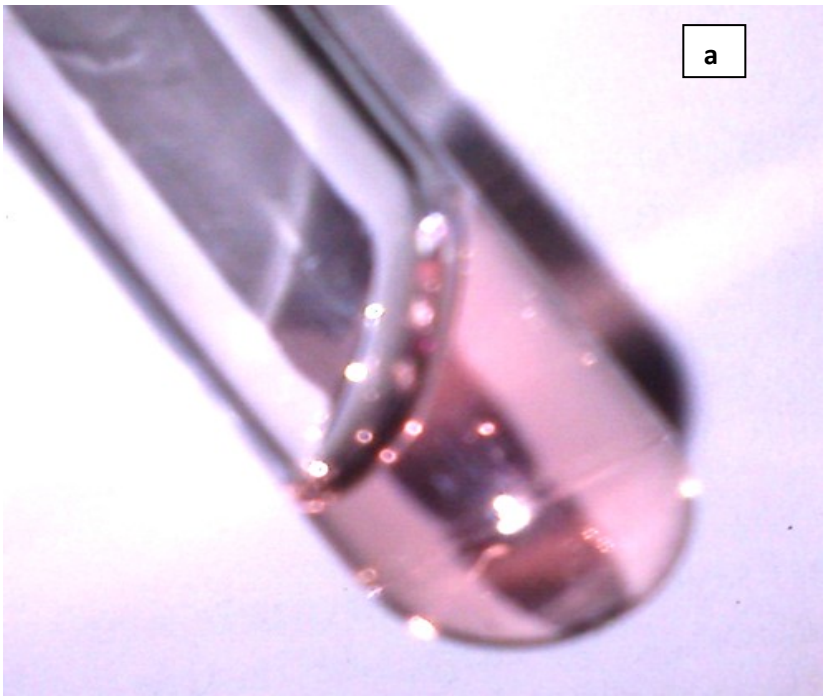

Fig 6. Free flowing pregel formulation (a), gel formed after crosslinking (shown in the inverted tissue culture tube) (b).

The viscosity of the injectable pregel formulations in water at 37 °C was determined to evaluate their applicability and feasibility as an injectable hydrogel *in vivo*. Data showed that viscosity values ranged between 40 - 42 centipoise (cP) (Table 5) for all three pregel formulations. Evidently, these values fall well below the U.S. FDA-approved permissible limit of ~50 cP for subcutaneous injectable systems (Shire *et al.*, 2004), which clearly demonstrates that pXMP polymers have great potential for use as injectable cell or drug delivery systems in various biomedical applications.

Table 5: viscosity of the injectable formulation

Injectable pregel formulation	Viscosity (cP)
P-R1	40
P-R2	40
P-R3	42

The optimum viscosity of these injectable pregel formulations lies within the FDA specification of 50 cp, which clearly reveals the suitability as injectable pregel formulation. The prepared hydrogels exhibited elastic properties and possessed good optical characteristics for light microscopy.

4.4.Characterisation of hydrogels

4.4.1 Swelling Studies

The equilibrium degree of swelling of the prepared XMP hydrogels was evaluated by incubating them in PBS or SBF at pH~7.4 for 24 h. The equilibrium swellings of swollen hydrogels with different prepolymers are shown in Figure 7.

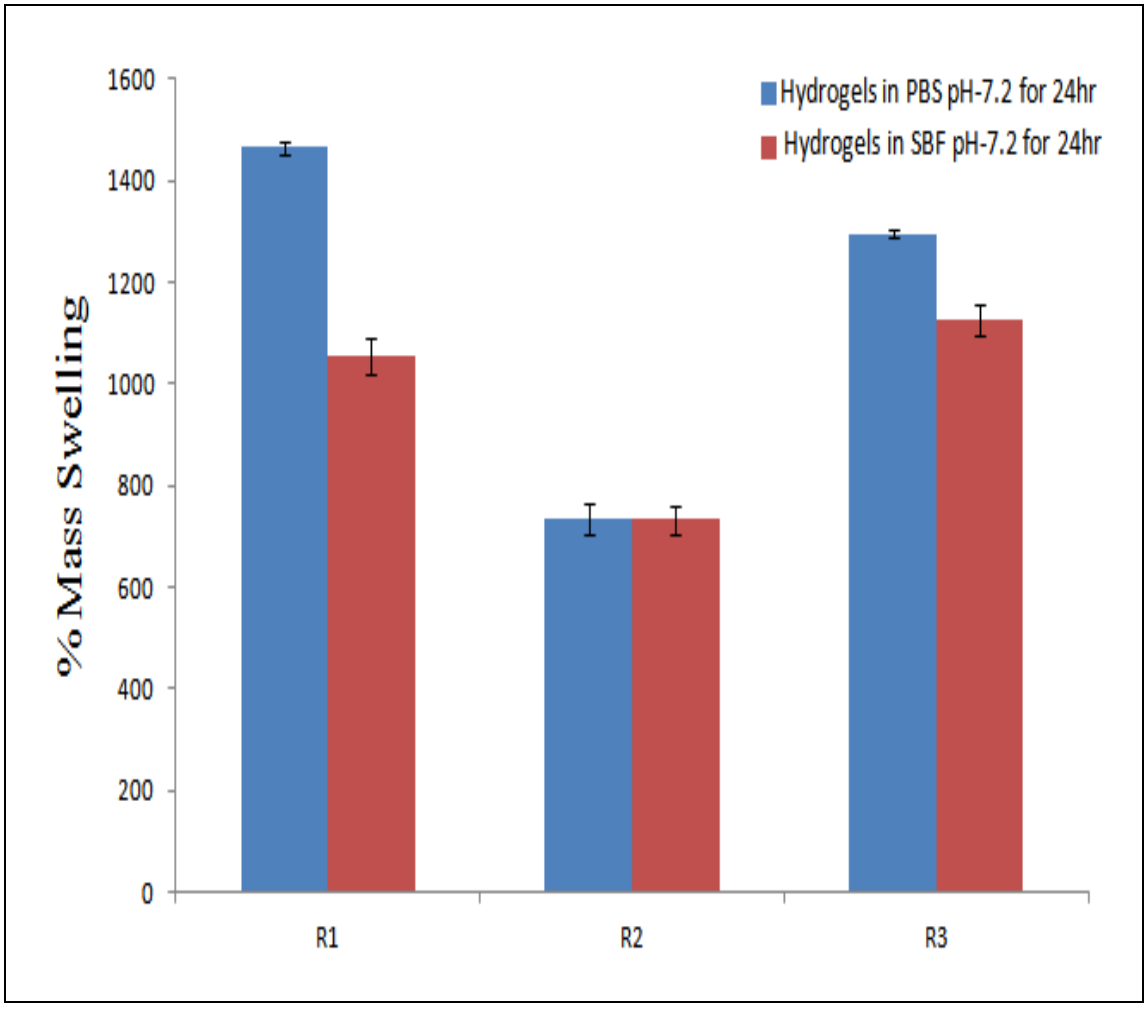

Fig. 7. Swelling studies of crosslinked hydrogels

The swelling behavior of hydrogels depends on the crosslinking density, number of polar -OH or -COOH groups present in the polymer network, as well as the ionic strength and pH of the surrounding medium. Swelling ratios were observed to be higher for hydrogels swollen in PBS compared to those in SBF, which clearly demonstrate the presence of ionizable pendant -COOH groups. Furthermore, R1 and R3 hydrogels exhibited significantly higher swelling ratios compared to R2 hydrogels. This could be attributed to the increased presence of freely available -OH groups in R1 or -COOH groups in R3, both of which have stoichiometric molar excess of xylitol or maleic acid compared to Xy/MA ratio of R2 gels. The average Crosslinking density (ζ) and molecular weight between crosslinks (*Mc)* of the present hydrogels ranged between 3.44 - 4.4 x 10^{-3} mol/cm^3 and 228 - 295, respectively (Figure 8).

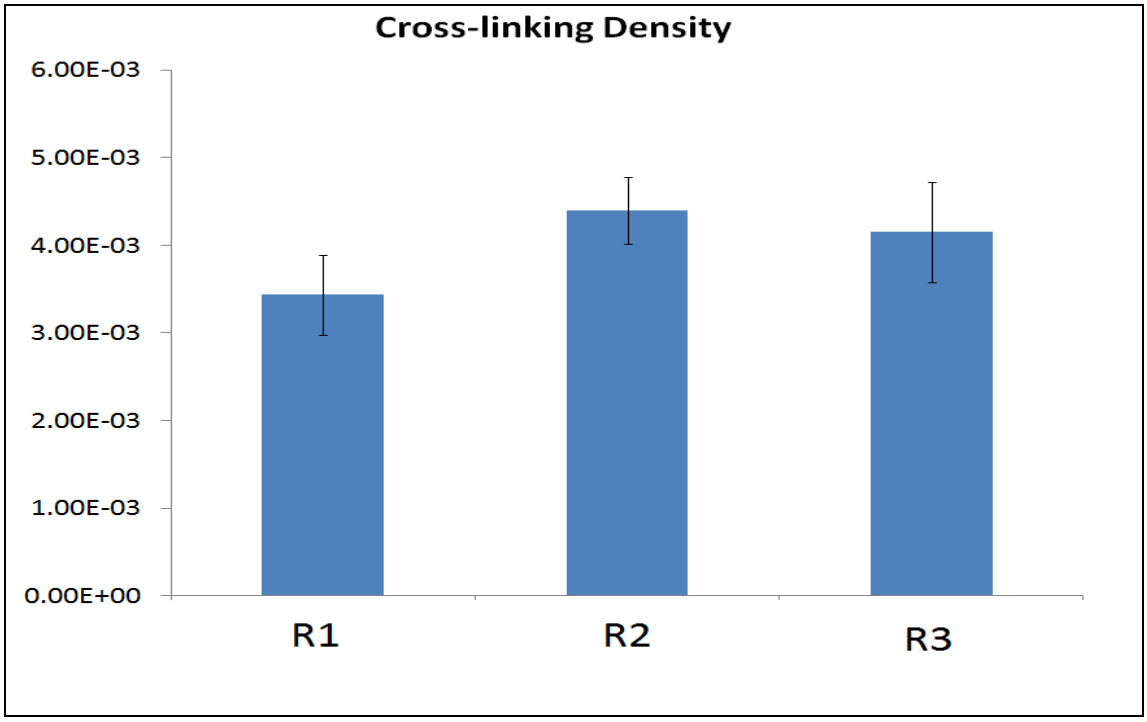

Fig.8. Crosslinking density of hydrogels

Crosslinking density (ζ) and molecular weight between crosslinks (*Mc)* are important factors that govern the physical properties of covalently crosslinked hydrogels. These parameters greatly influence the stability and biodegradation of hydrogels under physiological conditions in vivo. ζ and *Mc* of hydrogels were determined via swelling measurements in SBF *in vitro*. The crosslinking density (ζ) and molecular weight between crosslinks (*Mc)* values indicate that the synthesized pXMP hydrogels possess high degree of crosslink density, which in turn could lead to increased lifetime and long-term performance *in vivo*.

4.4.2 Dynamic contact angle studies

The dynamic contact angle (θ_w) measurements of pXMP-based hydrogels in water are presented in Table 6. The θ_w values for the synthesized pXMP hydrogels ranged from 82° - 95°. As θ_w in the range of 100°~150° are considered highly hydrophobic, the surfaces of synthesized hydrogels can be said to be mildly hydrophobic in nature. This observation is not uncharacteristic as surfaces of N-isopropylacrylamide nanocomposite hydrogels have been shown to be hydrophobic in spite of their hydrophilic constituents. Furthermore, a hydrophobic substrate is considered advantageous for cell encapsulation as they promote adsorption of extracellular matrix proteins that greatly influences cell adhesion and growth inside 3-D constructs. Interestingly, it was also observed that θ_w of present hydrogels showed a gradual but marginal decrease with increasing Xy/MA

ratios. This could be due to the steady incremental increase of free -OH groups which has been shown to influence substrate hydrophilicity.

Table 6. Physical properties of the pXMP hydrogels.

Hydrogels	Dynamic Contact Angles (°)		Max. Load	Max. Stress	Compression Young's Modulus
	Advancing	Receding	(N)	(KPa)	(KPa)
R1	94.81 ± 1.27	91.97 ± 0.57	0.8155	2.012	11.68
R2	93.36 ± 1.23	92.02 ± 0.48	5.272	19.452	117.58
R3	87.85 ± 6.87	82.25 ± 5.92	2.297	6.947	31.36

4.4.3. Mechanical testing

The mechanical properties of hydrogels should ideally match the modulus of target tissue to minimize tissue irritation and achieve successful integration with host tissue. R2 hydrogels with molar ratio of Xy/MA=0.2 exhibited significantly higher Young's modulus (117.58 ± 2.8KPa) and load at break (5.27 ± 0.34N) when compared to hydrogels that had a stoichiometric excess of maleic acid (Xy/MA < 0.2) or xylitol (Xy/MA > 0.2) (Table 3). R1

exhibited the lowest Young's modulus (11.68 ± 2KPa) and load at break (0.81 ± 0.23N) values while R3 hydrogels demonstrated a Young's modulus and load at break of 31.36 ± 1.871 KPa and 5.27 ± 1.4N, respectively.

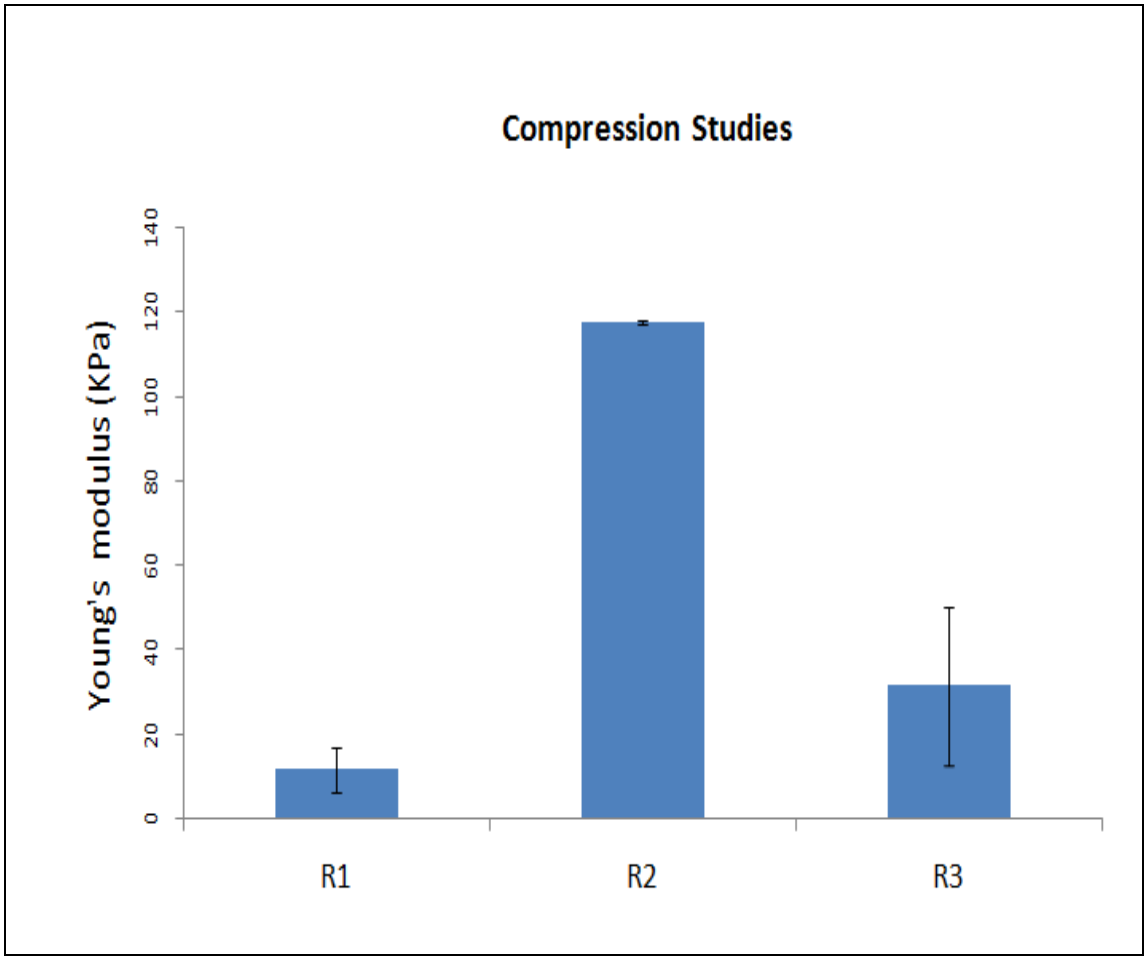

Fig.9. Compressive modulus of hydrogels in SBF

The compression data (Table 6, Figure 9) is also in good agreement with the measured swelling and crosslinking density values as low crosslinking densities or high swelling ratios is associated with longer polymer chains between crosslinks which substantially reduces the compressive strength of crosslinked gels. More importantly, it can be inferred that by

manipulating the ratio of Xy/MA, injectable pXMP-based hydrogels with broad range of compressive moduli can be designed to match the natural mechanical environment of various native tissues, including brain (0.1 - 1 KPa), muscle (8 - 17 KPa) and collagenous bone (100 KPa).

4.4.4. Degradation studies

Degradation profiles of the crosslinked hydrogels in PBS were recorded for a period 7 weeks. It was observed that 65% of mass was lost during the first week of the study. However, the percentage mass loss remained constant for the next 6 weeks with an average loss falling around 15% (Figure 10).

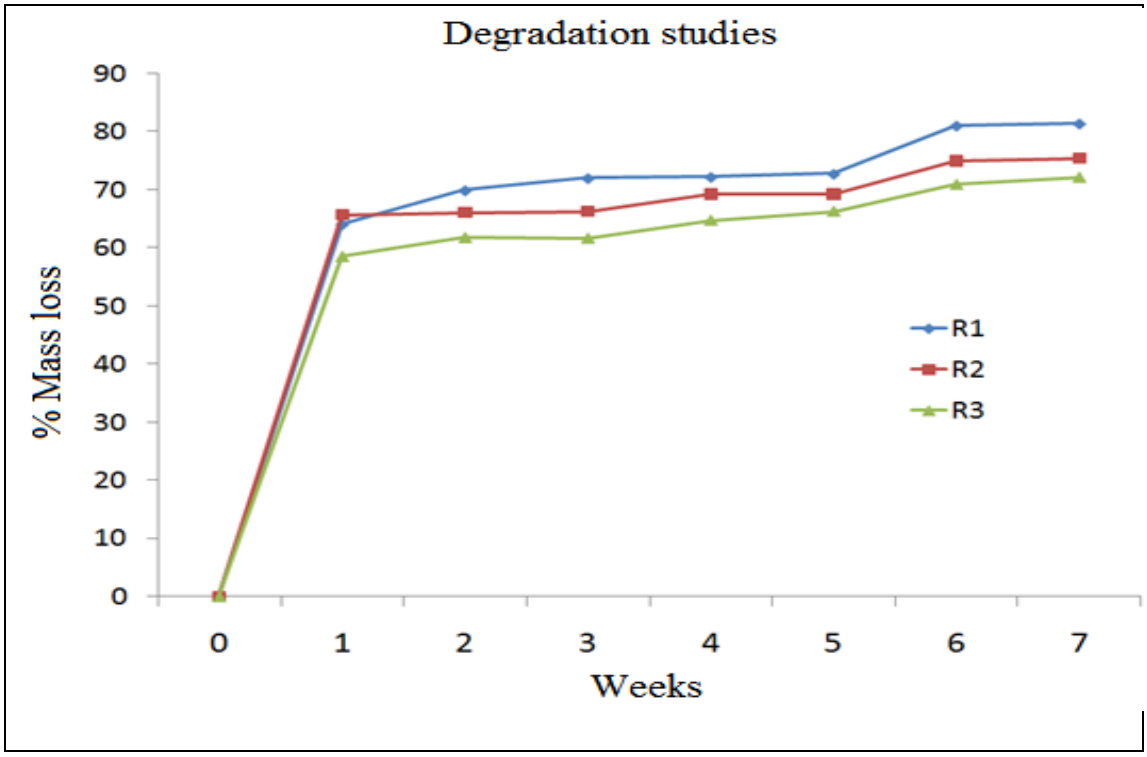

Fig.10. Degradation of hydrogels in PBS

4.4.5. SEM studies

The morphology of degraded hydrogels in PBS was also evaluated using SEM. SEM microgrpah of untreated hydrogel is given in figure 11. The SEM picture reveal surface without any cracks or pores. SEM microgrpahs of aged hydrogel in PBS for 4 and 35 days are given in figures 12 and 13. SEM micrographs showed that the hydrogels degraded rapidly during the first week and the % mass loss remained constant throughout the studied 7-week period.

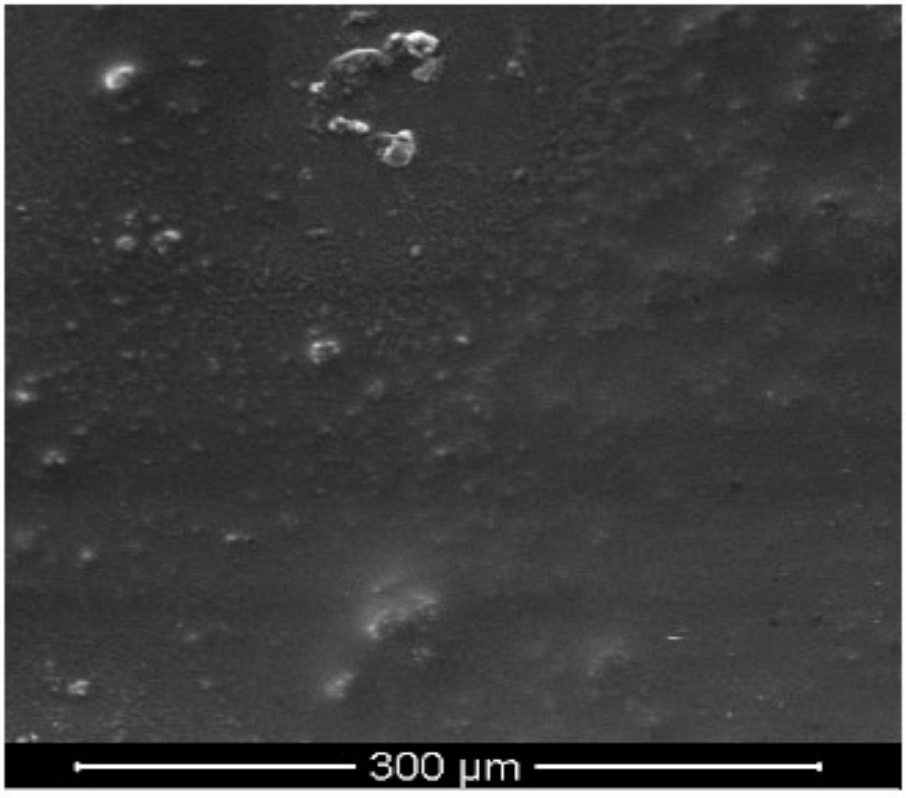

Fig. 11. ESEM image of untreated R3 hydrogel

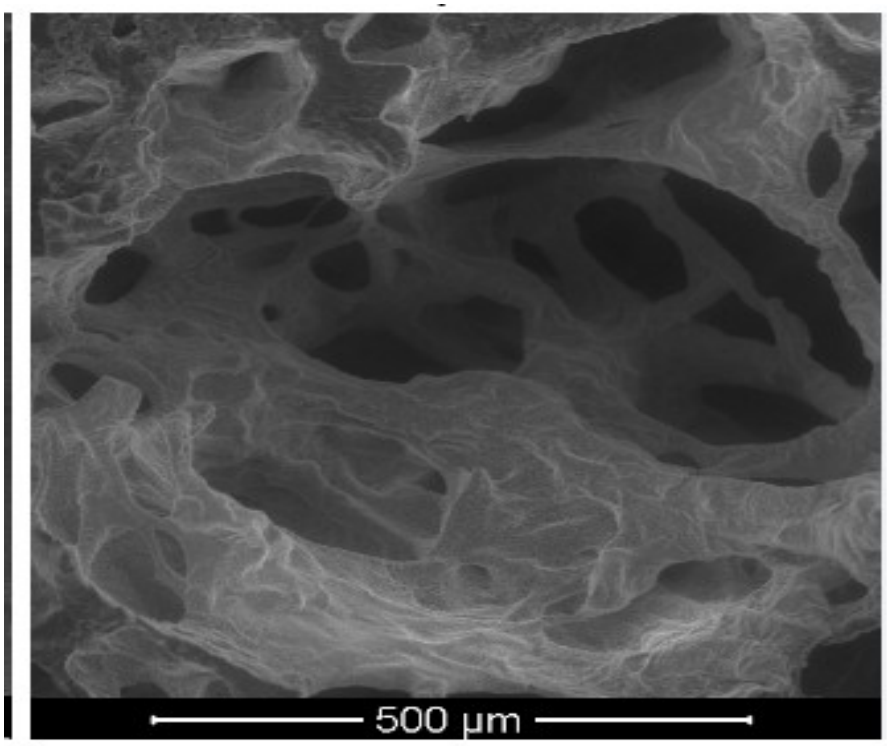

Fig. 12 ESEM image of aged R3 hydrogel in PBS for 4 days

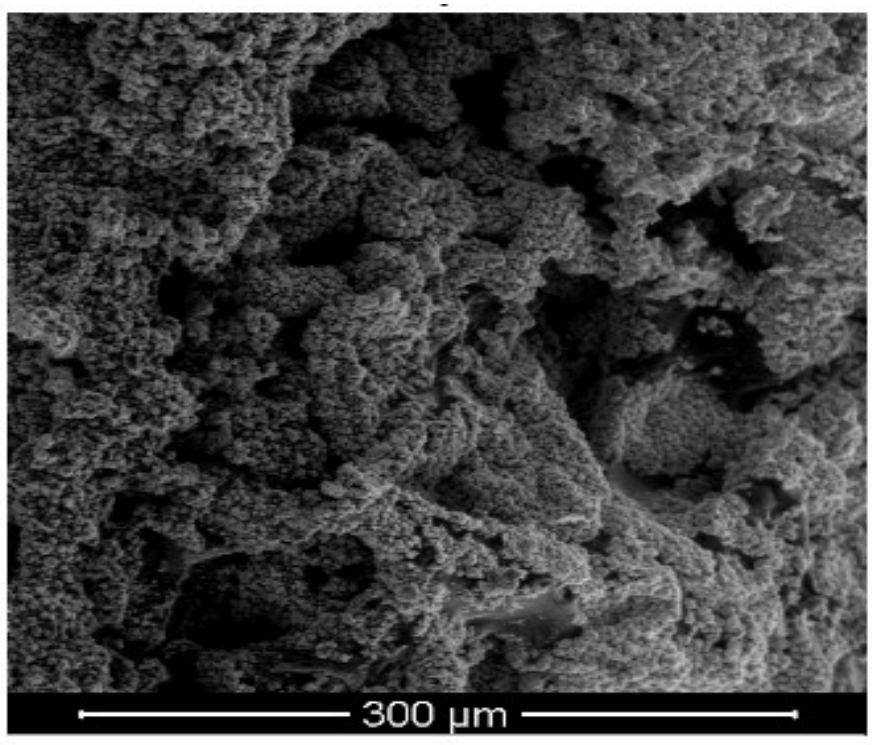

Fig. 13 ESEM image of aged R3 hydrogel in PBS for 7 weeks

4.5. Biological characterization of pXMP hydrogels

4.5.1. Protein adsorption studies

Protein-material interaction at the tissue-implant interface plays a crucial role in mediating initial cellular events that modulate host responses to an implanted biomaterial (Anderson, 2001). Furthermore, the nature and amount of blood plasma proteins adsorbed onto a material surface determines the biocompatibility of the implanted system (Winterton *et al*., 1986). Non-specific adsorption of albumin has been shown to promote implant surface "passivity" whereas fibrinogen has been attributed to implant thrombogenicity (Ji *et al*., 2001). Albumin adsorption from fresh human plasma on the surfaces of the present hydrogels was examined using SDS-PAGE analysis with protein bands identified and compared to standard plasma (Figure 14).

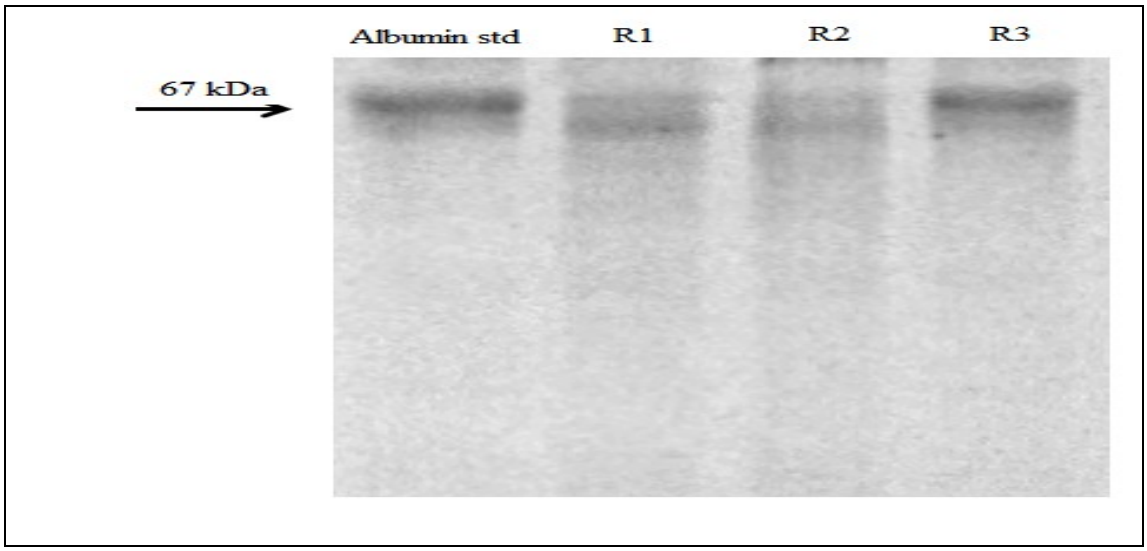

Fig. 14. Albumin adsorption on surfaces of the prepared hydrogels as evaluated by SDS-PAGE analysis.

Results from the densitometric scan clearly showed that all hydrogels exhibited preferential albumin adsorption when compared to other plasma proteins.

4.5.2. Cytotoxicity studies

Cytotoxicity testing is the first critical step to determine the biocompatibility of a material for clinical applications. The cytotoxicity evaluation was done to assess the potential of the hydrogel for cell encapsulation. The hydrogel samples were found to be non-cytotoxic upon contact with the L929 cells. Representative phase contrast photograph of fibroblasts cells around the R3 hydrogel is shown in figure. 15 ai and bi. The DAPI stained fluorescent images of the nucleus of the cells (figure. 15 aii and bii) suggest the viability of L929 cells in the hydrogel networks. MTT assay was performed to evaluate the acute cytotoxic effects of hydrogel degradation products and leachable components on L929 fibroblast cells (Figure 16).

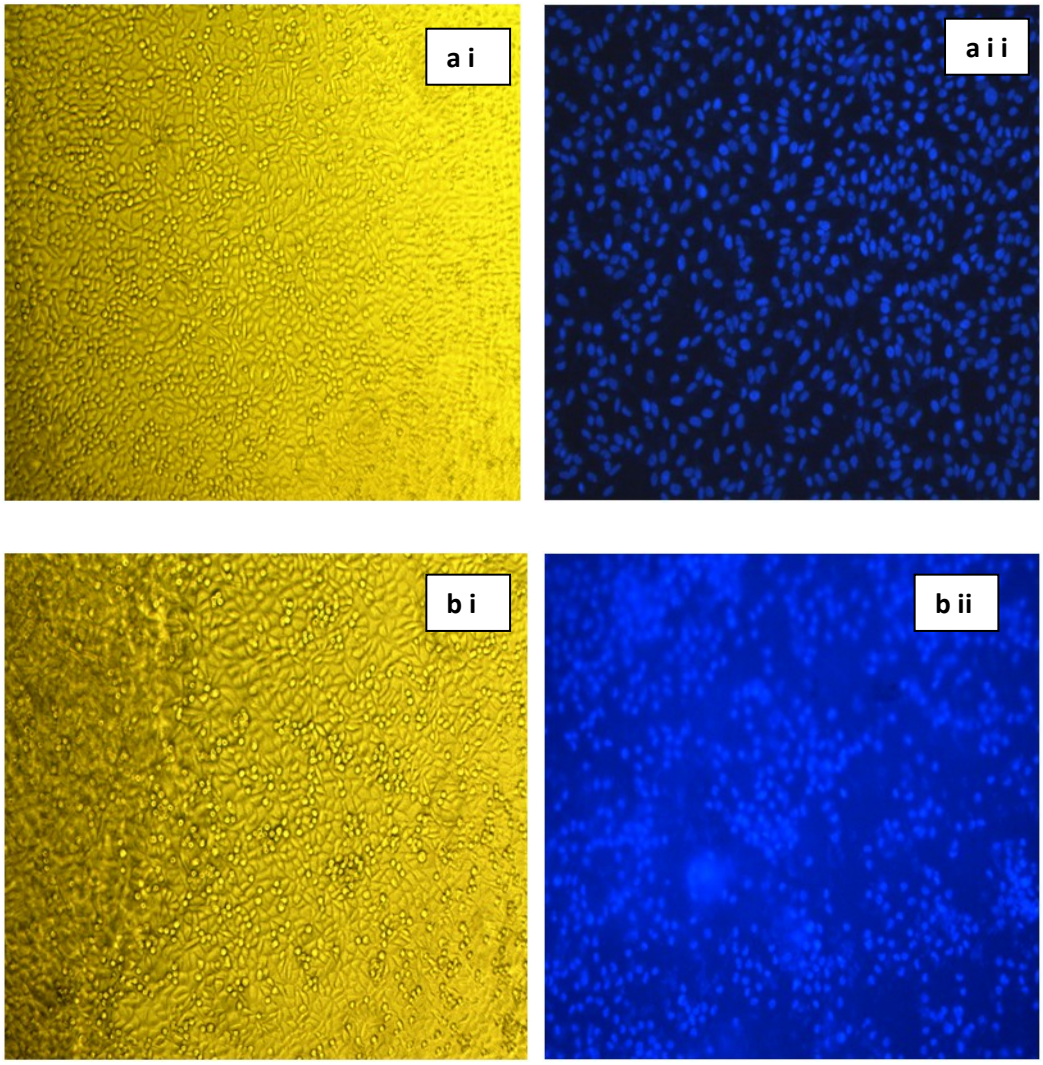

Fig.15.Phase contrast photograph (10X) of L-929 cells in direct contact with material. Control (ai), R3 hydrogel (bi). DAPI stained fluorescent image of L929 control (aii), R3 hydrogel (bii) (20X)

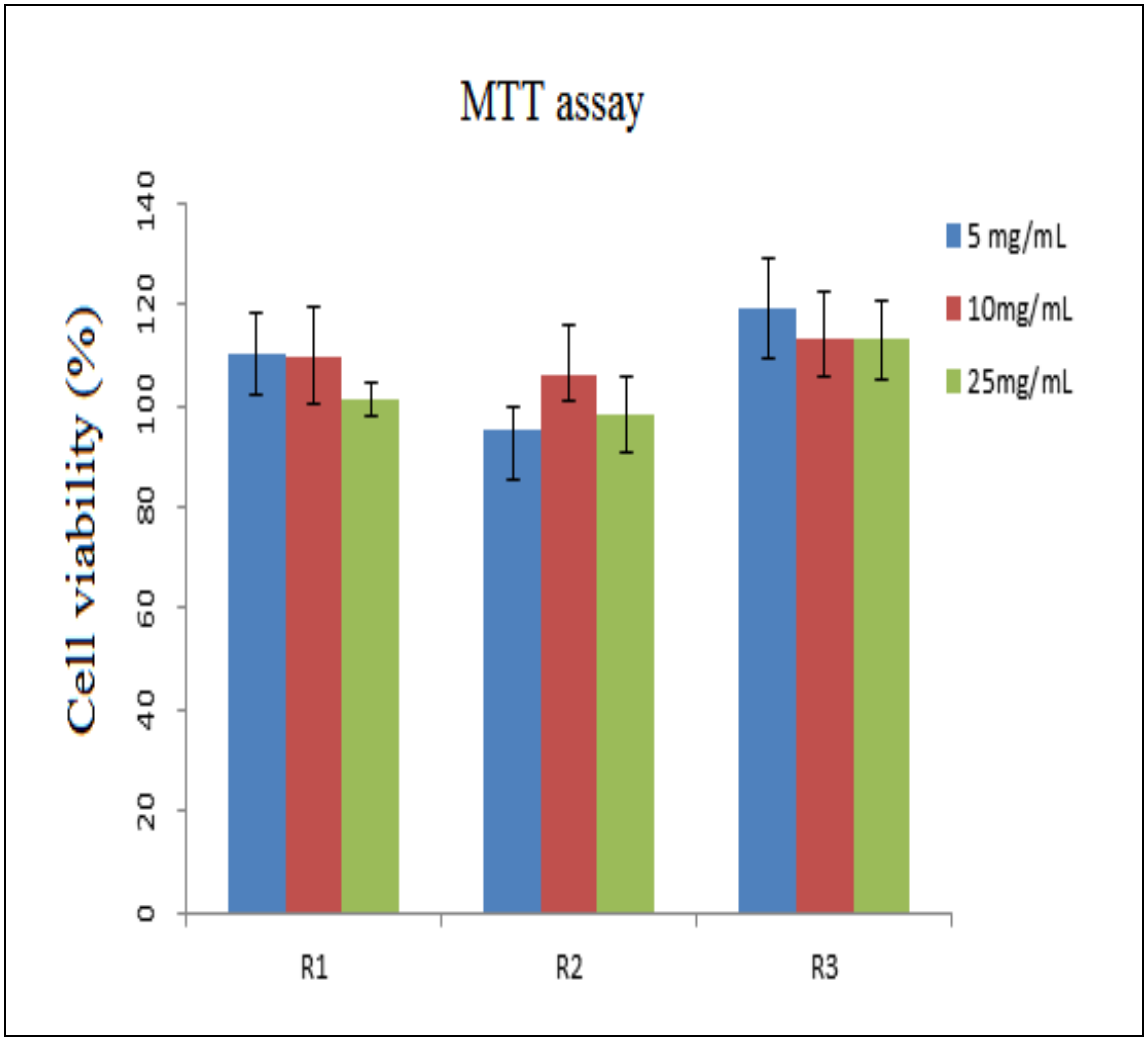

Fig.16. Cell viability of L929 cells with hydrogels

The assay revealed no appreciable toxicity at all three concentrations tested (5, 10 and 25 mg/ml), with hydrogels exhibiting >95% viability after a 24 h incubation period. These data suggest that the prepared pXMP hydrogels and their degradation products were non-toxic to cells *in vitro*.

4.6. Studies on cell encapsulation

The present encapsulation of L929 cells with hydrogel reveal infiltration of cells within the pores of the hydrogel. The phase contrast photograph of L-929 cells encapsulated in the R3 hydrogel is shown in figure 17. The cells looked round as they have to conform to the shape of pores as reported elsewhere (Julian Thiele et al 2014).

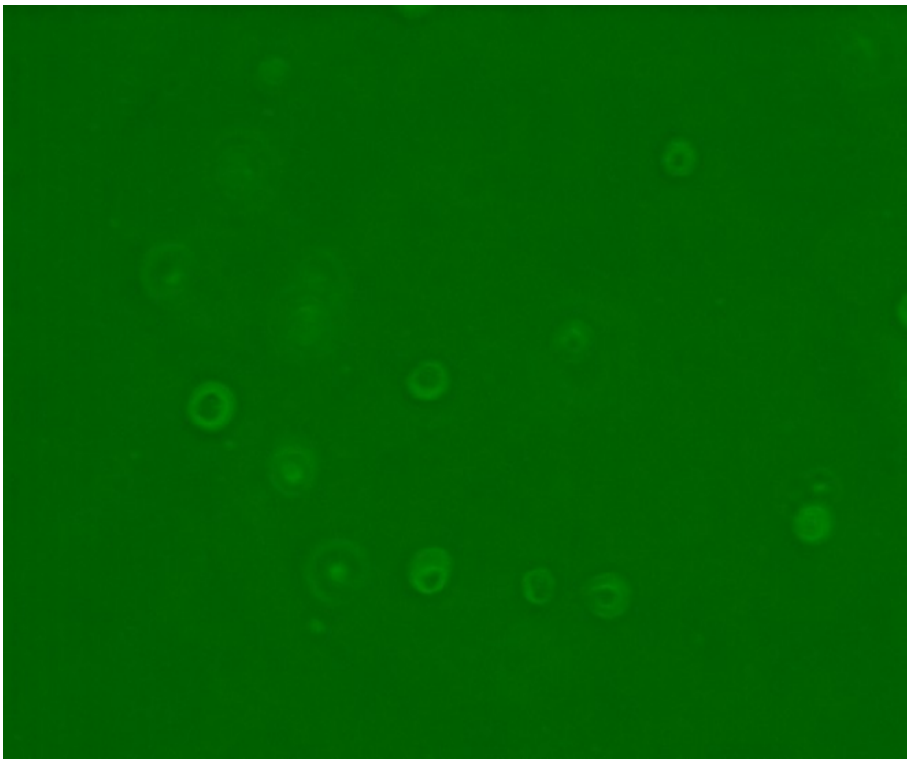

Fig.17.Phase contrast photograph (20X) of L-929 cells encapsulated in the R3 hydrogel

The live-dead assay of the encapsulated cells reveal viability of cells inside the hydrogel. The fluorescent microscopic analysis after live/dead staining using calcein displayed green fluorescence indicating the retention of nuclear integrity of the cells grown inside the hydrogels (Figure 18). The absence of high intensity red fluorescence with ethidium homodimer indicates the viability of the cells (Figure 19). This nuclear integrity is the sign of healthy and proliferating cells implying the cytocompatibility of the hydrogels and their ability to support cell growth and function. Moreover, this is the indication of the absence of apoptosis, anoikis and necrosis. Since calcein is a permeable dye, it can enter all the cells and makes the nuclei to fluoresce green.

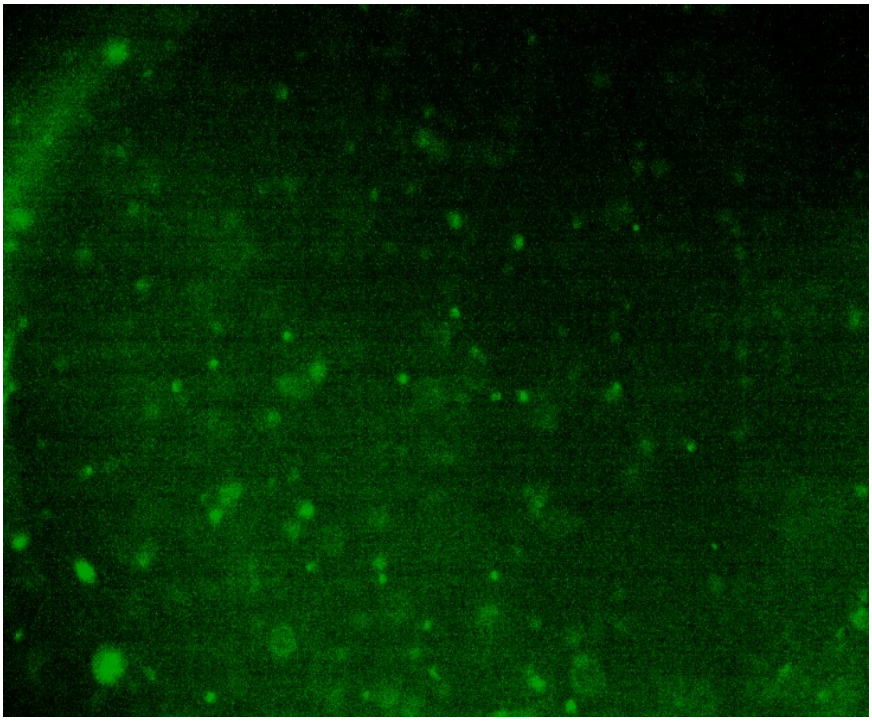

Fig.18. Fluorescent microscopic image after live/dead staining using calcein showing healthy encapsulated cells in R3 hydrogels

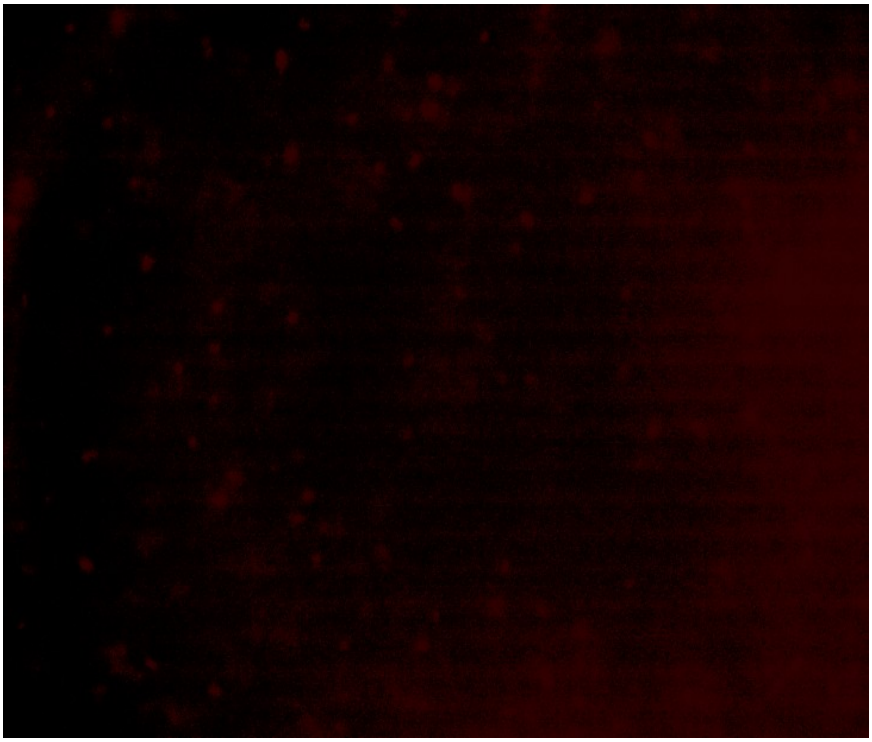

Fig.19. Fluorescent microscopic image after live/dead staining using ethidium homodimer showing poor number of dead cells in R3 hydrogels

5. CONCLUSIONS

We report the successful syntheses and characterization of *in situ* crosslinkable xylitol-PEG based pregel formulation for potential use as injectable hydrogels for cell delivery applications. The water-soluble prepolymer is synthesized using simple one-pot synthesis with xylitol, maleic acid and PEG as monomers by varying the mole ratio of xylitol and maleic acid. Further the pregel is evaluated for injectability and which lies within the FDA specified limits(i.e 50 cP). The FT-IR and H'NMR analyses reveal the formation of reactive functional fumarate groups and ester groups, C-C double bonds which can be crosslinked to form network. The analyses of molecular weights (number average, *Mn* and weight average, *Mw*) and polydispersity index of the synthesized pXMP prepolymers confirms the oligomeric nature of the prepolymer. The free flowing pregel formulations consisting xylitol-PEG prepolymer and acrylic acid with catalyst and accelerator have viscosity within the FDA-approved permissible limit of ~50 cP, which reveal easy injectability for cell or drug delivery systems

The hydrogels prepared with pregel formulation have higher swelling ratios in PBS compared to those in SBF. R1 and R3 hydrogels exhibited

significantly higher swelling ratios compared to R2 hydrogels. The variable swelling characteristics and cross-linking density emphasizes the applicability of the polymers for wide variety of applications. Moreover the present hydrogels have hydrophobic character. The R2 hydrogels with molar ratio of Xy/MA=0.2 exhibited significantly higher Young's modulus though other hydrogels that had a stoichiometric excess of maleic acid (Xy/MA < 0.2) or xylitol (Xy/MA > 0.2) exhibited lower mechanical strength. The mechanical study signified their applicability for wide range of tissues whose native mechanical strengths fairly fall in this range. The gradual degradation of hydrogels in PBS after 1 week as demonstrated by SEM studies suggests the appreciable stability in physiological conditions.

The protein adsorption studies reveal preferential albumin adsorption on the hydrogel when compared to other plasma proteins. The cytotoxicity assay with L929 fibroblast cells revealed that the present hydrogels and their degradation products were non-toxic to L929 cells *in vitro*.

A step ahead to further show the compatibility and delivery of cells using pXMP polymers is through direct cell encapsulation. In this study we demonstrated cell encapsulation with good viability after 24h.

The studies on the present hydrogels, prepared using three ratios of pXMP class prepolymers reveals the tunability and scalability nature. Further studies can be carried out by encapsulating various cell types according to the matching ECM properties of the cells to evaluate the formation of native tissue like constructs. Further drug delivery or cell delivery efficacy can be studied by carrying out invivo-studies. Collating all the properties together, this class of injectable hydrogel formulation can have promising application ranging from

injectable therapeutics to tissue engineered construct. Owing to the versatilie properties like low viscocity and high water solubility, it can be a promising candidate for development of engineered constructs using latest technologies like rapid prototyping, bioprinting, microfluidic encapsulation of single cells.

References

Annabi N., A. Tamayol, J. A. Uquillas, M. Akbari, L. E. Bertassoni, C. Cha, G. Camci-Unal, M. R. Dokmeci, N. a Peppas, and A. Khademhosseini, “25th Anniversary Article: Rational Design and Applications of Hydrogels in Regenerative Medicine.,” Adv. Mater. Res., vol. 26, no. 1, pp. 85–124, Jan. 2014.

Bruggeman J. P., C. J. Bettinger, and R. Langer, “Biodegradable xylitol-based elastomers: in vivo behavior and biocompatibility.,” J. Biomed. Mater. Res. A, vol. 95, no. 1, pp. 92–104, Oct. 2010.

Bruggeman J. P., C. J. Bettinger, C. L. E. Nijst, D. S. Kohane, and R. Langer, “Biodegradable Xylitol-Based Polymers,” Adv. Mater., vol. 20, no. 10, pp. 1922–1927, May 2008.

Cascone Maria Grazia, Lazzeri Luigi, Sparvoli Enzo, Scatena Manuele, Serino Lorenzo Pio, Danti Serena (2004) Morphological evaluation of bioartificial hydrogels as potential tissue engineering scaffolds. *J. Mater. Sci. Mater. Med.* 15: 1309–1313.

Frisman Ilya, Seliktar Dror, Bianco-Peled Havazelet (2012) Nanostructuring biosynthetic hydrogels for tissue engineering: a cellular and structural analysis. *Acta Biomater.* 8: 51–60.

Gayet JC, Fortier G (1995) Drug release from new bioartificial hydrogel. *Artif. Cells. Blood Substit. Immobil. Biotechnol.* 23: 605–611.

Gulrez S. K. H., S. Al-assaf, and G. O. Phillips, “Hydrogels : Methods of Preparation , Characterisation and Applications,” 2003.

Hoffman A. S., “Hydrogels for biomedical applications.,” Ann. N. Y. Acad. Sci., vol. 944, pp. 62–73, Nov. 2001.

Ito T. , Y. Yeo , C. B. Highley , E. Bellas , D. S. Kohane , *Biomaterials* **2007** , *28* , 3418

Jayabalan M, Thomas V, Sreelatha PK (2000) Studies on poly(propylene fumarate-co-ethylene glycol) based bone cement. *Biomed. Mater. Eng.* 10: 57–71.

Jayabalan M, Shalumon KT, Mitha MK (2009) Injectable biomaterials for minimally invasive orthopedic treatments. *J. Mater. Sci. Mater. Med.* 20: 1379–1387.

Ji J., L. Feng and M.A. Barbosa, *Biomaterials* **22**, 3015 (2001).

Julian Thiele, Yujie Ma, Designer hydrogels for cell cultures : A materials selection guide, Adv.Mater.2014, 26, 125-148.

Khetan S, Burdick J Cellular encapsulation in 3D hydrogels for tissue engineering, JoVE 2009, doi.10.3791/1590

Leach Jennie B, Schmidt Christine E (2005) Characterization of protein release from photocrosslinkable hyaluronic acid-polyethylene glycol hydrogel tissue engineering scaffolds. *Biomaterials* 26: 125–135.

Liu C., *J. Appl. Polym. Sci.* **2013** , *127* , 577 .

Li Zhenqing, Guan Jianjun (2011) Hydrogels for Cardiac Tissue Engineering. *Polymers* 3: 740–761.

Li Y., W. Huang, W. D. Cook, and Q. Chen, “A comparative study on poly(xylitol sebacate) and poly(glycerol sebacate): mechanical properties, biodegradation and cytocompatibility.,” Biomed. Mater., vol. 8, no. 3, p. 035006, Jun. 2013.

Loh Xian Jun, Li Jun (2007) Biodegradable thermosensitive copolymer hydrogels for drug delivery. *Expert Opin. Ther. Pat.* 17: 965–977.

Luo Y., J. B. Kobler , J. T. Heaton , X. Jia , S. M. Zeitels , R. Langer, *J. Biomed. Mater. Res. B. Appl. Biomater.* **2010** , *93* , 386

Mäkinen KK, Hämäläinen MM (1985) Metabolic effects in rats of high oral doses of galactitol, mannitol and xylitol. *J. Nutr.* 115: 890–899.

Martinez-Sanz E., D. A. Ossipov, J. Hilborn, S. Larsson, K. B. Jonsson, O. P. Varghese, *J. Controlled Release* **2011**, *152*, 232

Nguyen M. K. and D. S. Lee, “Injectable biodegradable hydrogels.,” Macromol. Biosci., vol. 10, no. 6, pp. 563–79, Jun. 2010.

Ossipov D. A., J. Hilborn , *Macromolecules* **2006** , *39* , 1709 .

Pal K., A. K. Banthia, M. Engineering, and P. Vihar, “Polymeric Hydrogels : Characterization and Biomedical Applications – A mini review,” vol. 12, pp. 197–220, 2009.

Patenaude M., N. M. B. Smeets, and T. Hoare, “Designing injectable, covalently cross-linked hydrogels for biomedical applications.,” Macromol. Rapid Commun., vol. 35, no. 6, pp. 598–617, Mar. 2014.

Peng G., J. Wang , F. Yang , S. Zhang , J. Hou , W. Xing , X. Lu , C. Liu , *J. Appl. Polym. Sci.* **2013** , *127* , 577

Rodrigues Y. Li, J., and H. Tomás, “Injectable and biodegradable hydrogels: gelation, biodegradation and biomedical applications.,” Chem. Soc. Rev., vol. 41, no. 6, pp. 2193–221, Mar. 2012.

Sailakshmi G, Mitra Tapas, Gnanamani A (2013) Engineering of chitosan and collagen macromolecules using sebacic acid for clinical applications. *Prog. Biomater.* 2: 1–12.

Saha N., “Polymeric Biomaterial Based Hydrogels for Biomedical Applications,” J. Biomater. Nanobiotechnol., vol. 02, no. 01, pp. 85–90, 2011.

Seliktar D., “Designing cell-compatible hydrogels for biomedical applications.,” Science, vol. 336, no. 6085, pp. 1124–8, Jun. 2012.

Serrano Maria Concepcion, Chung Eun Ji, Ameer Guillermo A (2010) Advances and Applications of Biodegradable Elastomers in Regenerative Medicine. *Adv. Funct. Mater.* 20: 192–208.

Shire, S.J., Shahrokh, Z., Liu, J. Challenges in the development of high protein concentration formulations (2004) *Journal of Pharmaceutical Sciences*, 93: 1390-1402.

Tran R., Y. Zhang, D. Gyawali, and J. Yang, "Recent Developments on Citric Acid Derived Biodegradable Elastomers," Recent Patents Biomed. Eng., vol. 2, no. 3, pp. 216–227, Nov. 2009.

Vercruysse K. P., D. M. Marecak , J. F. Marecek , G. D. Prestwich , *Bioconjug. Chem.* **1997** , *8* , 686

Wang Jane, Bettinger Christopher J, Langer Robert S, Borenstein Jeffrey T (2010) Biodegradable microfluidic scaffolds for tissue engineering from amino alcohol-based poly(ester amide) elastomers. *Organogenesis* 6: 212–216.

Welzel Petra Birgit, Prokoph Silvana, Zieris Andrea, Grimmer Milauscha, Zschoche Stefan, Freudenberg Uwe, Werner Carsten (2011) Modulating Biofunctional starPEG Heparin Hydrogels by Varying Size and Ratio of the Constituents. *Polymers* 3: 602–620.

Winterton L.C, J.D. Andrade, J. Feijen and S.W. Kim, *J. Colloidal Interfacial Sci.* **111**, 314 (1986).

Yu L. and J. Ding, "Injectable hydrogels as unique biomedical materials.," Chem. Soc. Rev., vol. 37, no. 8, pp. 1473–81, Aug. 2008.

List of Tables

List of Figures

10	Degradation of hydrogels in PBS
11	**ESEM image of untreated R3 hydrogel**
12	**ESEM image of aged R3 hydrogel in PBS for 4 days**
13	**ESEM image of aged R3 hydrogel in PBS for 7 weeks**
14	**Albumin adsorption on surfaces of the prepared hydrogels as evaluated by SDS-PAGE analysis.**
15	**Phase contrast photograph of L-929 cells in direct contact with material.**
16	**Cell viability of L929 cells with hydrogels**
17	**Phase contrast photograph of L-929 cells encapsulated in the R3 hydrogel**
18	**Fluorescent microscopic image after live/dead staining using calcein showing healthy encapsulated cells in R3 hydrogels**
19	**Fluorescent microscopic image after live/dead staining using ethidium homodimer showing poor number of dead cells in R3 hydrogels**